NATIONAL ADVISORY COMMITTEE FOR AERONAUTICS

TECHNICAL NOTE 2411

METHOD OF DETERMINING INITIAL TANGENTS OF CONTOURS OF FLOW VARIABLES BEHIND A CURVED, AXIALLY SYMMETRIC SHOCK WAVE

By George P. Wood and Paul B. Gooderum

Langley Aeronautical Laboratory
Langley Field, Va.

Washington
July 1951

NATIONAL ADVISORY COMMITTEE FOR AERONAUTICS

TECHNICAL NOTE 2411

METHOD OF DETERMINING INITIAL TANGENTS OF CONTOURS OF FLOW VARIABLES BEHIND A CURVED, AXIALLY SYMMETRIC SHOCK WAVE

By George P. Wood and Paul B. Gooderum

SUMMARY

A general method for calculating the initial tangents of contours of constant density, pressure, and Mach number behind a curved, axially symmetric shock wave has been derived. Initial tangents of density contours are obtained that fair well into contours determined from interferograms for the flow about a sphere at Mach number 1.62. Streamlines and contours of constant Mach number throughout this flow field have also been deduced from contours of constant density obtained by interferometry. The flow field obtained from the shock wave by the method of characteristics is compared with that obtained by interferometry.

INTRODUCTION

Various phases of the problem of flows behind curved shock waves have been treated theoretically by many investigators. Crocco, in a pioneer paper (reference 1), investigated two-dimensional flow behind a curved attached shock wave. Significant contributions were made later by Maccoll, Drougge, and Guderley. Maccoll (reference 2) calculated the flow around various bodies with detached shock waves at near-sonic velocities. Drougge (reference 3) calculated the pressure distribution on conical tips with detached shock waves. Guderley (reference 4) investigated the transition between flow with a detached shock wave and flow with an attached shock wave. Thomas, in a series of papers of which reference 5 is representative, considered the curvature of attached shock waves and the pressure distribution on bodies behind attached shock waves. Lin and Rubinov (reference 6) obtained general relations for flow behind curved shock waves and developed a method for calculating the subsonic flow between the shock wave and the body. This method was applied by Dugundji (reference 7) to calculate the pressure distribution along the axis between a sphere and a shock wave. Busemann (reference 8) reviewed analytical methods for the treatment of two-dimensional flows with detached shock waves and discussed the main features of mixed

subsonic and supersonic flows. Ferri (reference 9) presented a method for obtaining the pressure drag in two-dimensional or axially symmetric flow behind a detached shock wave when the location and shape of the shock wave are known. Moeckel (reference 10) gave an approximate method for predicting the form and the location of detached shock waves.

Experimental investigations of the flow behind curved shock waves include the investigation by Ladenburg, Van Voorhis, and Winckler (reference 11) who determined the density contours around various axially symmetric bodies at Mach number 1.7. The present authors in reference 12 presented data on the shape and location of detached shock waves on cones and spheres over a range of Mach numbers from 1.17 to 1.81. In reference 13 interferograms of the flow around a sphere at Mach numbers 1.30 and 1.62 were evaluated; the contours of constant density ratio in the flow field around the sphere were determined. However, the initial tangents of the density contours could not be obtained accurately from the interferogram by the method of analyzing interferograms that was used in reference 13.

The purpose of the present paper is to present a method for calculating the initial tangents of the contours of flow variables immediately behind a curved, axially symmetric shock wave when the location and shape of the shock wave are known. This method was used in the present paper to obtain the initial tangents of the density contours in the flow field around a sphere at Mach number 1.62. Streamlines and contours of constant Mach number in the flow behind the shock wave have also been obtained from the density contours of reference 13. The flow field in part of the supersonic region behind the shock wave has been computed by the method of characteristics (reference 14) and the results compared with those obtained from the interferogram.

SYMBOLS

a	velocity of sound
A	cross-sectional area
b	coordinate in plane of binormal
c_p	specific heat at constant pressure
c_v	specific heat at constant volume
D	diameter of sphere

F	distance to focus of streamline directions due to curvature of shock wave
log	logarithm to base e
M	Mach number
n	coordinate normal to direction of streamline
p	pressure
R	radius of curvature of streamline
R_w	radius of curvature of shock wave
S	entropy
ΔS	change in entropy $(S - S_0)$
t	coordinate tangential to direction of streamline
T	total taper distance of element of stream tube
T_b	taper distance of element of stream tube in plane of binormal
T_n	taper distance of element of stream tube in plane of normal
V	velocity
x	coordinate in direction of axis of symmetry
y	coordinate normal to axis of symmetry
γ	ratio of specific heats (c_p/c_v)
δ	angle of deviation of flow across shock wave
ϵ	angle of shock wave
θ_M	angle between direction of x-axis and initial tangent of contour of constant Mach number
θ_p	angle between direction of x-axis and initial tangent of contour of constant pressure

θ_ρ angle between direction of x-axis and initial tangent of contour of constant density

Π ratio of stagnation pressures $\left(p_s/p_{s_0}\right)$

ρ density

σ coordinate along shock wave

Subscripts:

s stagnation

0 free stream

SHOCK WAVE

In order to apply the method of calculating the initial tangents, that is developed in the present paper, the location of the shock wave and the variation along the shock wave of both the slope and the radius of curvature along the shock wave must be known. When the location and the slope variation of the shock wave are known, the streamlines can be obtained and the method of characteristics can be used to determine the flow field. The present section, therefore, is a discussion of the shock wave, its first and second derivatives, and its radius of curvature.

Figure 1, which is taken from figure 4(b) of reference 13, is the interferogram from which the coordinates of the bow shock wave and the other experimental results are obtained. This interferogram shows the flow about a sphere at a free-stream Mach number of 1.62. The free-stream stagnation temperature was 533.1° F absolute, and the free-stream density was 0.003501 slug per cubic foot. The rim shock wave from the edge of the nozzle is shown in the upper left-hand corner of the interferogram. This shock wave is very weak, as the fringe displacement across the shock wave is very small and the shock wave lies within 1° of the Mach angle. Because of the rim shock wave, however, and the nearness of the edge of the jet, the portion of the bow wave of the sphere between the rim shock wave and the edge of the jet was considered to be not sufficiently accurate and was not used (except for calculating one of the initial tangents; namely, the contour of constant density ratio of 1.5). The location of the portion of the bow shock wave between the rim shock wave and a position near the axis of symmetry was carefully measured and is shown in figure 2, where y is the normal distance from the axis of symmetry, x is the distance along the axis from the intersection of the shock wave and the axis, and D is the diameter of the

sphere. Because of the difficulty of making very accurate measurements near the axis where the slope of the shock wave is very large, the part of the shock wave near the axis has been shown as a dashed line.

The variation of the slope of the shock wave is given in figure 3. This curve was obtained by first reading y at values of x that increased by steps of 0.1, and then determining Δy, the increment in y for the given increment Δx in x. Next $\Delta x/\Delta y$ was plotted against y. The value of x was computed by finding the area under each small portion of the curve. If the value of x so obtained checked closely with the measured value of x, within approximately one part in a thousand, then the curve of $\Delta x/\Delta y$ was taken to be correct. If the check was not close, the curve was refaired until a close check was obtained. Then points were read from the curve of $\Delta x/\Delta y$ and were used for plotting the curve of dy/dx shown in figure 3.

The variation of d^2y/dx^2 was obtained in a similar manner. The quantity $\frac{\Delta x}{\Delta(\Delta y/\Delta x)}$ was plotted against $\frac{\Delta y}{\Delta x}$ and the curve was refaired until integration gave the original value of x within approximately three parts in a thousand. The variation of $-\left(\frac{d^2y}{dx^2}\right)D$ with $\frac{x}{D}$ is shown in figure 4.

From the variation of the first and the second derivatives, the variation of the radius of curvature of the shock wave was calculated. The radius of curvature obtained by this method, however, is not very accurate. Errors in the location and in the slope of the shock wave are magnified in the second derivative and, therefore, in the radius of curvature. In order to reduce the uncertainty in the radius, the shock wave on the other side of the axis (most of which is not shown in fig. 1, but which is included in the original interferogram from which fig. 1 was taken) was measured and its derivative and radius were calculated and plotted. The radius agreed fairly well with that obtained for the other side of the axis. Furthermore, with a mechanical device and a very large reproduction of the interferogram, the normals to the shock wave, the envelope of the normals, and then the variation of the radius of curvature along the shock wave were obtained. These results agreed rather well with the calculated values. A curve showing the variation of the radius of curvature along the shock wave that results from fairing through the measured points and the calculated points on both sides of the axis is given in figure 5.

RESULTS AND DISCUSSION

Initial Tangents of Contours of Flow Variables

In reference 13 the interferogram of figure 1 was analyzed to obtain the contours of constant density behind the shock wave. These contours are shown in figure 6, which is taken from figure 5(b) of reference 13. As was explained in reference 13, the analysis did not give accurately the contours in the region immediately behind the shock wave. For that reason there was a gap in figure 6 between the beginning of each contour and the known theoretical point where the shock wave and the contour should intersect. The purpose of the present section is to fill in these gaps by giving the theoretical values of the tangents of the contours at the shock wave.

The analysis for finding the initial tangents of the flow variables is given in detail in appendix A; however, the method is described briefly in the present section. The pressure immediately behind a curved shock wave varies along the shock wave. The rate of variation is obtained by differentiating along the shock wave the well-known equation for the pressure ratio across an oblique shock wave. The general rate of pressure change in any direction at any place in the flow field - including the one along a shock wave - may be represented by the two basic pressure derivatives, namely, in the direction of the tangent to the stream tube and in the direction of the normal to the stream tube. Therefore, the rate of pressure change along the shock wave is (appendix A)

$$\frac{d \log p}{d\sigma} = \cos(\epsilon - \delta) \frac{\partial \log p}{\partial t} + \sin(\epsilon - \delta) \frac{\partial \log p}{\partial n} \qquad (1)$$

Equation (1), with known values of ϵ, δ, and $\frac{d \log p}{d\sigma}$, is one relation between the two pressure derivatives. Another relation is also needed.

The tangential rate of change of pressure results from the tangential rate of change of velocity that is necessary to meet the requirement of continuity when there is a change in the cross-sectional area of the flow, and is given by Newton's second law of motion as

$$\frac{\partial p}{\partial t} = -\rho V \frac{\partial V}{\partial t}$$

or

$$\frac{\partial \log p}{\partial t} = \frac{\gamma M^2}{1 - M^2} \frac{\partial \log A}{\partial t} \tag{2}$$

The other basic rate of change is normal to the flow and balances the centrifugal force

$$\frac{\partial p}{\partial n} = - \frac{\rho V^2}{R}$$

or

$$\frac{\partial \log p}{\partial n} = - \frac{\gamma M^2}{R} \tag{3}$$

An equation that relates the two pressure derivatives can be obtained from equations (2) and (3) by finding the relation between $\frac{\partial \log A}{\partial t}$ and R, as follows: At every point on the shock wave, the local slope of the shock wave determines the initial streamline direction behind the shock wave. Inasmuch as there is always a point at the shock wave where the streamlines have no initial curvature, that point may be used for orientation, and the initial tangents of the streamlines may be considered rather than the streamlines themselves. Because the shock wave is curved, successive initial tangents of the streamlines behind the shock wave are not parallel and, therefore, if extended, converge to a focus (or in larger extent to an envelope) in the focal distance F (fig. 7). If the streamlines were straight, the focal distance F would determine the rate of change of cross-sectional area of the stream tubes and the rate of pressure change along the stream tube. Contours of constant pressure would be concentric circles around the focus (or the evolutes of the envelope). Since the pressure at the shock wave is known and since the entropy is known and is constant along a stream tube, there are two independent ways of calculating the rate of pressure change along the stream tube, one from the given pressure contours and the other from continuity inside the stream tube. These two methods, however, will agree for the tentatively straight streamlines only when the curvature of the shock wave and the distance from the axis of symmetry happen to have, fortuitously, the necessary values for agreement. In all other cases, a finite initial curvature of the streamlines has to modify the rate of change of area and to shift the contours of constant pressure in such a way that the two methods give the same result. In figure 8 the initial curvature of a streamline is indicated. In appendix A the details are given of finding the relation between the initial radius of curvature R of the streamline and the rate of change

of area of the stream tube. This relation is then used with equations (2) and (3) to obtain the following equation between the two pressure derivatives:

$$\frac{\partial \log p}{\partial n} = -\gamma M^2 \tan(\epsilon - \delta) \left[\frac{M^2 - 1}{\gamma M^2} \frac{\partial \log p}{\partial t} + \frac{\sin \delta}{y} + \csc(\epsilon - \delta) \frac{d\delta}{d\sigma} \right] \quad (4)$$

Equations (1) and (4) form a system of two equations in two unknowns and can be solved for the unknowns, the pressure derivatives. Then the effect of entropy variation along the shock wave can be taken into account to obtain expressions for the density derivatives and the Mach number (or temperature) derivatives.

When the two derivatives of a flow variable are known at a point on the shock wave in perpendicular directions, they can be added vectorially to find the direction of the maximum rate of change of the variable. Normal to that direction, then, is the direction of zero rate of change, which defines the tangent of the contour of constant value for the variable under consideration.

The final results are given by the three following equations, in which θ is the angle between the direction of the x-axis and the initial tangent of the contour of constant value of the variable indicated by the subscript on θ (the angle θ is considered positive when measured counterclockwise from the direction of the x-axis):

$$\frac{(\tan \theta_p - \delta)}{\tan(\epsilon - \delta)} = \frac{\frac{R_w}{y} \sin(\epsilon - \delta) \sin \delta + \frac{1}{\gamma M^2} \cot(\epsilon - \delta) \frac{\partial \log p}{\partial \epsilon} + \frac{\partial \delta}{\partial \epsilon}}{\frac{R_w}{y} \sin(\epsilon - \delta) \sin \delta + \frac{M^2 - 1}{\gamma M^2} \tan(\epsilon - \delta) \frac{\partial \log p}{\partial \epsilon} + \frac{\partial \delta}{\partial \epsilon}} \quad (5)$$

$$\frac{\tan(\theta_\rho - \delta)}{\tan(\epsilon - \delta)} = \frac{\frac{R_w}{y}\sin(\epsilon-\delta)\sin\delta + \frac{1}{\gamma M^2}\cot(\epsilon-\delta)\frac{\partial \log p}{\partial \epsilon} + \frac{\partial \delta}{\partial \epsilon}}{\frac{R_w}{y}\sin(\epsilon-\delta)\sin\delta + \frac{M^2-1}{\gamma M^2}\tan(\epsilon-\delta)\frac{\partial \log p}{\partial \epsilon} + \frac{\partial \delta}{\partial \epsilon} - \frac{\gamma-1}{\gamma}\frac{1-(M^2-1)\tan^2(\epsilon-\delta)}{M^2\tan(\epsilon-\delta)}\frac{\partial \log \Pi}{\partial \epsilon}} \tag{6}$$

$$\frac{\tan(\theta_M - \delta)}{\tan(\epsilon - \delta)} = \frac{\frac{R_w}{y}\sin(\epsilon-\delta)\sin\delta + \frac{1}{\gamma M^2}\cot(\epsilon-\delta)\frac{\partial \log p}{\partial \epsilon} + \frac{\partial \delta}{\partial \epsilon}}{\frac{R_w}{y}\sin(\epsilon-\delta)\sin\delta + \frac{M^2-1}{\gamma M^2}\tan(\epsilon-\delta)\frac{\partial \log p}{\partial \epsilon} + \frac{\partial \delta}{\partial \epsilon} + \frac{1-(M^2-1)\tan^2(\epsilon-\delta)}{\gamma M^2\tan(\epsilon-\delta)}\frac{\partial \log \Pi}{\partial \epsilon}} \tag{7}$$

The points on the shock wave where the contours of constant density should intersect the shock wave are known from the shock-wave angle. The directions of the tangents of the density contours have been calculated for these points by equation (6). The results are shown in the following table, which gives the value of the density ratio for a contour, the point on the shock wave where the contour should meet the shock wave, and the calculated values of θ_ρ at that point:

Density ratio, ρ/ρ_0	x/D	θ_ρ (deg)
2.0	0.046	64
1.9	.097	39
1.8	.168	11
1.7	.309	-27
1.6	.508	-70
1.5	.823	-95

The tangents are also indicated in figure 6 by the short, straight lines that have been drawn through the shock wave. The initial tangents given by the analysis fit well between the experimentally determined contours and the known points where the contours should intersect the shock wave.

Streamlines and Contours of Constant Mach Number Determined from Density Contours

The only known quantity in the flow field behind the shock wave, except at the shock wave and at the surface of the sphere, is the density, as given in figure 6. The values of the other state variables of the gas are not immediately known because of the variation along the shock wave of the entropy behind the shock wave. The streamlines, as the contours of constant entropy, can be found, however, by a graphical method that is based on satisfying continuity along a stream tube. The local cross-sectional area of a stream tube can be expressed, if its entropy is given, in terms of known quantities in the free stream and the local values of density and stagnation density. The first stream tube is constructed by taking the axis and the surface of the sphere as a streamline. Local values of density, as given by figure 6, and the average value of stagnation density for the stream tube are used to calculate local values of cross-sectional area. Then, adjacent stream tubes are added in sequence. The method is described in detail in appendix B.

From the steamlines and the density contours, the other flow variables can be found. In the present case, the contours of constant Mach number were found. The results are shown in figure 9, where the density contours taken from figure 6 are shown by the heavy solid lines, the streamlines, by the light solid lines, and the calculated Mach number contours, by the dashed lines.

Streamlines and Contours of Constant Density and Mach Number Determined by Method of Characteristics

Contours of the flow variables in part of the flow field behind the shock wave were calculated by the method of characteristics. The part of the flow field for which results can be obtained is quite limited in extent. The flow field is limited on one side by the subsonic flow in front of the sphere and on the other side by the fact that the location and shape of the bow shock wave are not known accurately enough for use beyond the nozzle-rim shock wave. The method used was that given by Ferri (reference 14). The only data needed for the calculations were the free-stream conditions, the coordinates of the shock

wave (fig. 2), and the variation of the slope of the shock wave (fig. 3). The calculations were made with the Bell Telephone Laboratories X-66744 relay computer at the Langley Laboratory. An attempt to obtain good accuracy in the results was made by using fairly small increments (Δy on the shock wave approximately equal to 0.04D) to give a network of characteristics that had a small mesh and by reiterating each step of the process. The results are shown in figure 10. Contours of constant ratio of density to free-steam density are shown in figure 10(a), where the contours obtained by interferometry are also reproduced from figure 6. Contours of constant Mach number are shown in figure 10(b), which also shows the Mach number contours obtained by satisfying continuity, transferred from figure 9. Streamlines, or contours of constant entropy, obtained by the method of characteristics are shown in figure 10(c), together with those taken from figure 9.

The contours obtained by the method of characteristics and the contours obtained from the interferogram do not agree very well. Actually, however, the agreement is perhaps as good as might be expected. In deriving an axially symmetric flow field from experimental measurements, results that have an extremely high degree of accuracy are difficult to obtain. In the present case, the results obtained by the method of characteristics have some small percentage of uncertainty because of the finite size of the mesh of the characteristics network. The analysis of an interferogram of axially symmetric flow must also be made very carefully in order to obtain results in which the uncertainty is very small. In reference 13, from which the interferometric results were taken, the estimate is made that the uncertainty in the location of any contour does not exceed plus or minus approximately one-half the distance between the adjacent contours. This amount of uncertainty, which is only about 3 percent, is just about equal to the discrepancy between the results obtained by the two methods.

The fact that the streamlines are straight in the only region of the flow in which the method of characteristics could be applied is entirely fortuitous in the sense that the curvature of the shock wave and the distance to the axis for this region are such that the streamlines are straight.

CONCLUDING REMARKS

A method of calculating the initial tangents of contours of constant density, pressure, and Mach number at a curved symmetrical shock wave has been derived. The method gives tangents of density contours that fair well between the contours obtained by interferometry and the known points of intersection on the shock wave.

The streamlines of the flow about a sphere at Mach number 1.62 have been deduced from experimentally determined density contours by satisfying the requirements of continuity along a stream tube.

Part of the flow field around the sphere was also obtained from a knowledge of the shock wave by applying the method of characteristics.

Langley Aeronautical Laboratory
National Advisory Committee for Aeronautics
Langley Field, Va., April 12, 1951

APPENDIX A

CALCULATION OF INITIAL TANGENTS OF CONTOURS OF FLOW VARIABLES

The problem is to find the tangents of the contours of constant pressure, density, and Mach number immediately behind an axially symmetric curved shock wave. The solution given here was obtained by using ideas and suggestions of Dr. A. Busemann of the Langley Laboratory.

A curved, axially symmetric shock wave in a uniform, steady, supersonic free steam is considered. The location of such a shock wave can, because of axial symmetry, be completely given by two variables, and the shock wave can be drawn as a curve in a meridian plane. The local slope of the shock wave with respect to the free-stream direction of flow, together with the state of the gas in the free stream, completely determines the initial state of the gas and the initial tangent to the direction of the streamline at any and every point on the downstream side of the shock wave. In particular, the pressure is given by the equation

$$\frac{p}{p_0} = \frac{2\gamma}{\gamma + 1} M_0^2 \sin^2 \epsilon - \frac{\gamma - 1}{\gamma + 1} \tag{A1}$$

Because the shock wave is curved, the local slope, the flow variables, and the initial tangent to the streamlines vary along the shock wave. In particular, the rate of change of pressure along the shock wave is obtained from equation (A1) as

$$\frac{d \log p}{d\sigma} = \frac{d\epsilon}{d\sigma} \frac{2\gamma M_0^2 \sin \epsilon \cos \epsilon}{\gamma M_0^2 \sin^2 \epsilon - \frac{\gamma - 1}{2}} \tag{A2}$$

Another way of viewing the pressure change along the shock wave is the following: The rate of pressure change in any direction at any point in a flow field - for example, along a shock wave - is the sum of the components in that direction of the two basic rates of change. One of these basic rates of pressure change lies in the direction tangent to the direction of flow. This tangential rate of change results from any tangential rate of change of velocity that may be necessary to meet the requirements of continuity when there is a change in the cross-sectional area of the flow. It is given by Newton's second law of motion as

$$\frac{\partial p}{\partial t} = - \rho V \frac{\partial V}{\partial t}$$

By using the relations

$$M^2 = V^2 \frac{\partial \rho}{\partial p}$$

and

$$M^2 = \frac{\rho V^2}{\gamma p}$$

the equation can be written as

$$\frac{\partial \log p}{\partial t} = \frac{\gamma M^2}{1 - M^2} \frac{\partial \log A}{\partial t} \tag{A3}$$

The other basic rate of pressure change is normal to the flow direction, balances centrifugal force, and is

$$\frac{\partial p}{\partial n} = - \frac{\rho V^2}{R}$$

or

$$\frac{\partial \log p}{\partial n} = - \frac{\gamma M^2}{R} \tag{A4}$$

At any point on the shock wave, the rate of change of pressure along the downstream side of the shock wave is the sum of the components along the shock wave of $\partial p/\partial t$ and $\partial p/\partial n$, that is,

$$\frac{d \log p}{d\sigma} = \cos(\epsilon - \delta) \frac{\partial \log p}{\partial t} + \sin(\epsilon - \delta) \frac{\partial \log p}{\partial n} \tag{A5}$$

Another relation between $\frac{\partial \log p}{\partial t}$ and $\frac{\partial \log p}{\partial n}$ is needed. This relation can be obtained by finding first a geometrical relation between $\frac{\partial \log A}{\partial t}$ and R, the unknown factors in equations (A3) and (A4). Consider first a section of the flow as seen in a meridian plane (fig. 7). Because the shock wave is curved, the initial tangents to the streamlines behind the shock wave change along the shock wave. The initial tangents, therefore, if extended, converge to an envelope or focus, in the focal distance F. In the general case, the stream tube is not identical with the extended initial tangents that converge in the distance F, since the stream tube is curved in the meridian plane. If, however, the streamlines were straight, the distance F to the focus would be one of the factors that determine the rate of change of area of the stream tube, as this distance would define the taper of the stream-tube area in the meridian plane. The taper of a stream tube as

seen in a meridian plane is, however, not the only taper. Consider an element of an annular axially symmetric stream tube as shown in figure 11. The cross-sectional area of the element is

$$dA = dn\ db$$

The element tapers not only in the meridian plane, which is the plane of the normal, but also in the plane of the binormal. In other words, both dn and db vary along the stream tube. The quantity db is proportional to y as shown in figure 11. If the cross section under consideration were moved away from the shock wave, y and db would become larger. If the cross section were moved in the opposite direction, db would become smaller at a rate that would make it vanish at the axis of symmetry. The side of the element in the plane of the binormal therefore would taper to an edge or focus at the axis in the distance $-T_b = \frac{y}{\sin \delta}$.

The total taper of the element of stream tube is made up of the components in the plane of the normal and in the plane of the binormal. The total taper of the element could then be considered as having an envelope distance T, and would be given by

$$\frac{1}{T} = \frac{1}{F} + \frac{1}{T_b} = -\frac{dA}{A\ dt} \tag{A6}$$

(where straight streamlines in the meridian plane are assumed).

If the local Mach number in the element of stream tube were unity, the cross-sectional area of the element would be constant, dA/dt would be zero, and the normal and the binormal tapers would be opposite and equal $\left(F = -T_b\right)$. At a Mach number of 1 behind the shock wave, however, $d\delta/d\sigma$ is almost equal to zero for a perfect gas and the distance F is not equal to $-T_b$. In fact, F is greater than $-T_b$. In order, therefore, for the taper in the plane of the normal to have the correct value of

$$-T_b = \frac{y}{\sin \delta}$$

the streamline must have an initial concave curvature at the shock wave, as shown in figure 12. The initial tangent on one side of the stream tube and the tangent at the opposite point of the stream tube, which is at a distance dt from the shock wave, are extended and intersect at the taper distance T_n. For a Mach number of 1 the requirement is, therefore, that

$$T_n = -T_b$$

and the streamlines must have a curvature to meet this requirement. In the general case, also, of Mach number other than unity, the envelope distance given by

$$F = -\frac{dn}{d\delta}$$

at the shock wave is not the correct taper in the plane of the normal, but is either too large or too small, and the streamline must have an initial concave or convex curvature. The component of taper in the meridian plane is defined by a different pair of tangents from the initial tangents. The taper is always T_n, as shown, but in the general case T_n is not equal to $-T_b$.

The relation between the radius of curvature R and the taper distance T_n can be obtained from figure 12, as follows: δ varies both along σ and along t. The angle subtended by dt is $\frac{d\delta}{dt}\,dt$. The angle subtended by dn is $-\frac{d\delta}{d\sigma}\,d\sigma + \frac{d\delta}{dt}\,dt$. The two triangles with $\frac{d\delta}{dt}\,dt$ as vertex angle are similar, therefore

$$\frac{dt}{R} = \frac{dn + T_n \frac{d\delta}{d\sigma}\,d\sigma}{T_n} = \frac{dn}{T_n} + d\delta$$

or

$$\frac{1}{R} = \tan(\epsilon - \delta)\,\frac{1}{T_n} + \sec(\epsilon - \delta)\,\frac{d\delta}{d\sigma}$$

This relation can now be used to obtain the relation between $1/R$ and $\frac{\partial \log A}{\partial t}$.

Equation (A6) can now be rewritten as

$$\frac{1}{T_n} = \frac{1}{T} - \frac{1}{T_b} = -\frac{dA}{A\,dt} + \frac{\sin\delta}{y}$$

Therefore

$$\frac{1}{R} = \tan(\epsilon - \delta)\left(\frac{-dA}{A\,dt} + \frac{\sin\delta}{y}\right) + \sec(\epsilon - \delta)\,\frac{d\delta}{d\sigma}$$

$$= \tan(\epsilon - \delta)\left[\frac{-dA}{A\,dt} + \frac{\sin\delta}{y} + \csc(\epsilon - \delta)\,\frac{d\delta}{d\sigma}\right] \qquad (A7)$$

Equation (A7) is the relation between $1/R$ and $\frac{\partial \log A}{\partial t}$ that was needed to obtain another relation between the pressure derivatives by using equations (A3) and (A4). If $1/R$ as given by equation (A7) is substituted in equation (A4), then

$$\frac{\partial \log p}{\partial n} = -\gamma M^2 \tan(\epsilon - \delta)\left[\frac{\sin \delta}{y} - \frac{dA}{A\,dt} + \csc(\epsilon - \delta)\frac{d\delta}{d\sigma}\right] \tag{A8}$$

If $\frac{\partial \log A}{\partial t}$ is eliminated between equations (A8) and (A3), then

$$\frac{\partial \log p}{\partial n} = -\gamma M^2 \tan(\epsilon - \delta)\left[\frac{\sin \delta}{y} + \frac{M^2 - 1}{\gamma M^2}\frac{\partial \log p}{\partial t} + \csc(\epsilon - \delta)\frac{d\delta}{d\sigma}\right] \tag{A9}$$

Solution of equations (A5) and (A9) for the two rates of change of pressure gives

$$\frac{\partial \log p}{\partial t} = \frac{\gamma M^2 \tan^2(\epsilon - \delta)}{1 - (M^2 - 1)\tan^2(\epsilon - \delta)}\left[\frac{\sin \delta}{y} + \frac{1}{\gamma M^2}\frac{\cot(\epsilon - \delta)}{\sin(\epsilon - \delta)}\frac{d \log p}{d\sigma} + \csc(\epsilon - \delta)\frac{d\delta}{d\sigma}\right]$$

$$\frac{\partial \log p}{\partial n} = \frac{-\gamma M^2 \tan(\epsilon - \delta)}{1 - (M^2 - 1)\tan^2(\epsilon - \delta)}\left[\frac{\sin \delta}{y} + \frac{M^2 - 1}{\gamma M^2}\sec(\epsilon - \delta)\frac{d \log p}{d\sigma} + \csc(\epsilon - \delta)\frac{d\delta}{d\sigma}\right]$$

By use of the relations

$$n = y \sec \delta$$

$$R_w = \frac{d\sigma}{d\epsilon}$$

and

$$\frac{d}{d\sigma} = \frac{\partial}{\partial \epsilon}\frac{d\epsilon}{d\sigma}$$

$$= \frac{1}{R_w}\frac{\partial}{\partial \epsilon}$$

the pressure derivatives can be written

$$\frac{\frac{\partial \log p}{\partial t}}{n} = \frac{\gamma M^2 \tan^2(\epsilon - \delta)}{1 - (M^2 - 1)\tan^2(\epsilon - \delta)} \left[\tan \delta + \frac{1}{\gamma M^2} \frac{n}{R_w} \frac{\cot(\epsilon - \delta)}{\sin(\epsilon - \delta)} \frac{\partial \log p}{\partial \epsilon} + \frac{\dot{n}}{R_w} \csc(\epsilon - \delta) \frac{\partial \delta}{\partial \epsilon} \right] \tag{A10}$$

$$\frac{\partial \log p}{\partial \log n} = \frac{-\gamma M^2 \tan(\epsilon - \delta)}{1 - (M^2 - 1)\tan^2(\epsilon - \delta)} \left[\tan \delta + \frac{M^2 - 1}{\gamma M^2} \frac{n}{R_w} \sec(\epsilon - \delta) \frac{\partial \log p}{\partial \epsilon} + \frac{n}{R_w} \csc(\epsilon - \delta) \frac{\partial \delta}{\partial \epsilon} \right] \tag{A11}$$

The next step is to find the direction in which dp is zero. This direction is that along which the components of the tangential and the normal pressure derivatives are equal in magnitude and opposite in sign. If θ_p is the angle between this direction and the x-axis, then $\tan(\theta_p - \delta)$ is given by the ratio of $\frac{\partial \log p}{\partial t}$ to $\frac{-\partial \log p}{\partial n}$. Therefore

$$\frac{\tan(\theta_p - \delta)}{\tan(\epsilon - \delta)} = \frac{\frac{R_w}{y} \sin(\epsilon - \delta) \sin \delta + \frac{1}{\gamma M^2} \cot(\epsilon - \delta) \frac{\partial \log p}{\partial \epsilon} + \frac{\partial \delta}{\partial \epsilon}}{\frac{R_w}{y} \sin(\epsilon - \delta) \sin \delta + \frac{M^2 - 1}{\gamma M^2} \tan(\epsilon - \delta) \frac{\partial \log p}{\partial \epsilon} + \frac{\partial \delta}{\partial \epsilon}} \tag{A12}$$

The problem that has been solved herein for axially symmetric flow has previously been solved by Lin and Rubinov (reference 6) for plane flow. Reference 6 also gives the fundamental equations for conservation of mass, momentum, and energy in axially symmetric flow. As a check on the results obtained in the present paper, equations (A10) and (A11), the present authors have done the following: By starting with the fundamental conservation equations for axially symmetric flow as given in reference 6, and by using only algebraic manipulation, as was used in reference 6 for the plane case, expressions for the two pressure derivatives were obtained. These expressions were identical with those derived in the present paper as equations (A10) and (A11).

The expressions for pressure derivatives are converted into expressions for density and Mach number derivatives by taking into account changes in entropy:

$$p = e^{\Delta S/c_v} \rho^{\gamma}$$

$$\log p = \frac{\Delta S}{c_v} + \gamma \log \rho$$

But

$$c\Delta S = -(c_p - c_v) \log \Pi$$

Therefore

$$\log p = -(\gamma - 1) \log \Pi + \gamma \log \rho$$

$$\frac{\partial \log \rho}{\partial t} = \frac{1}{\gamma} \frac{\partial \log p}{\partial t} + \frac{\gamma - 1}{\gamma} \frac{\partial \log \Pi}{\partial t}$$

Tangent to a streamline, $\frac{\partial \log \Pi}{\partial t}$ is zero. Therefore

$$\frac{\frac{\partial \log \rho}{\partial t}}{n} = \frac{M^2 \tan^2(\epsilon - \delta)}{1 - (M^2 - 1)\tan^2(\epsilon - \delta)} \left[\tan \delta + \right.$$

$$\left. \frac{1}{\gamma M^2} \frac{n}{R_w} \frac{\cot(\epsilon - \delta)}{\sin(\epsilon - \delta)} \frac{\partial \log p}{\partial \epsilon} + \frac{n}{R_w} \csc(\epsilon - \delta) \frac{\partial \delta}{\partial \epsilon} \right] \qquad (A13)$$

Normal to a streamline,

$$\frac{\partial \log \rho}{\partial \log n} = \frac{1}{\gamma}\frac{\partial \log p}{\partial \log n} + \frac{\gamma - 1}{\gamma}\frac{\partial \log \Pi}{\partial \log n}$$

$$= \frac{1}{\gamma}\frac{\partial \log p}{\partial \log n} + \frac{\gamma - 1}{\gamma}\csc(\epsilon - \delta)\frac{n}{R_w}\frac{\partial \log \Pi}{\partial \epsilon}$$

$$= -\frac{M^2\tan(\epsilon - \delta)}{1 - (M^2 - 1)\tan^2(\epsilon - \delta)}\left[\tan\delta + \frac{M^2 - 1}{\gamma M^2}\frac{n}{R_w}\sec(\epsilon - \delta)\frac{\partial \log p}{\partial \epsilon} + \right.$$

$$\left.\frac{n}{R_w}\csc(\epsilon - \delta)\frac{\partial \delta}{\partial \epsilon}\right] + \frac{\gamma - 1}{\gamma}\frac{n}{R_w}\csc(\epsilon - \delta)\frac{\partial \log \Pi}{\partial \epsilon} \qquad \text{(A14)}$$

Equations (A13) and (A14) give the density derivatives tangent and normal to a streamline. Figure 13 shows the variation of the two derivatives with x/D.

The angle of the contour of constant density is then given by the equation

$$\frac{\tan\left(\theta_\rho - \delta\right)}{\tan(\epsilon - \delta)} = \frac{\frac{R_w}{y}\sin(\epsilon - \delta)\sin\delta + \frac{1}{\gamma M^2}\cot(\epsilon - \delta)\frac{\partial \log p}{\partial \epsilon} + \frac{\partial \delta}{\partial \epsilon}}{\frac{R_w}{y}\sin(\epsilon - \delta)\sin\delta + \frac{M^2 - 1}{\gamma M^2}\tan(\epsilon - \delta)\frac{\partial \log p}{\partial \epsilon} + \frac{\partial \delta}{\partial \epsilon} - \frac{\gamma - 1}{\gamma}\frac{1 - (M^2 - 1)\tan^2(\epsilon - \delta)}{M^2\tan(\epsilon - \delta)}\frac{\partial \log \Pi}{\partial \epsilon}} \tag{A15}$$

The variation of θ_ρ with x/D is shown in figure 14. Furthermore

$$p_s = p\left(1 + \frac{\gamma - 1}{2}M^2\right)^{\frac{\gamma}{\gamma - 1}}$$

and therefore

$$d \log M = \frac{1 + \frac{\gamma - 1}{2}M^2}{\gamma M^2}\left(d \log \Pi - d \log p\right)$$

Consequently the two Mach number derivatives are

$$\frac{\frac{\partial \log M}{\partial t}}{n} = -\frac{\left(1 + \frac{\gamma - 1}{2}M^2\right)\tan^2(\epsilon - \delta)}{1 - \left(M^2 - 1\right)\tan^2(\epsilon - \delta)}\left[\tan\delta + \frac{1}{\gamma M^2}\frac{n}{R_w}\frac{\cot(\epsilon - \delta)}{\sin(\epsilon - \delta)}\frac{\partial \log p}{\partial \epsilon} + \frac{n}{R_w}\csc(\epsilon - \delta)\frac{\partial \delta}{\partial \epsilon}\right]$$

$$\frac{\partial \log M}{\partial \log n} = \frac{\left(1 + \frac{\gamma - 1}{2} M^2\right)\tan(\epsilon - \delta)}{1 - \left(M^2 - 1\right)\tan^2(\epsilon - \delta)} \left[\tan \delta + \frac{M^2 - 1}{\gamma M^2} \frac{n}{R_w} \sec(\epsilon - \delta) \frac{\partial \log p}{\partial \epsilon} + \right.$$

$$\left. \frac{n}{R_w} \csc(\epsilon - \delta)\frac{\partial \delta}{\partial \epsilon}\right] + \frac{1 + \frac{\gamma - 1}{2} M^2}{\gamma M^2} \frac{n}{R_w} \frac{1}{\sin(\epsilon - \delta)} \frac{\partial \log \Pi}{\partial \epsilon}$$

Then

$$\frac{\tan(\theta_M - \delta)}{\tan(\epsilon - \delta)} = \frac{\frac{R_w}{y} \sin(\epsilon - \delta) \sin \delta + \frac{1}{\gamma M^2} \cot(\epsilon - \delta) \frac{\partial \log p}{\partial \epsilon} + \frac{\partial \delta}{\partial \epsilon}}{\frac{R_w}{y} \sin(\epsilon - \delta) \sin \delta + \frac{M^2 - 1}{\gamma M^2} \tan(\epsilon - \delta) \frac{\partial \log p}{\partial \epsilon} + \frac{\partial \delta}{\partial \epsilon} + \frac{1 - \left(M^2 - 1\right)\tan^2(\epsilon - \delta)}{\gamma M^2 \tan(\epsilon - \delta)} \frac{\partial \log \Pi}{\partial \epsilon}} \tag{A16}$$

For use in the final equations (A14) to (A16), the value of ϵ for a given value of ρ/ρ_0 was found from the equation

$$\sin^2\epsilon = \frac{\rho/\rho_0}{\left(\frac{\gamma + 1}{2}\right)M_0^2 - \left(\frac{\gamma - 1}{2}\right)M_0^2 \frac{\rho}{\rho_0}}$$

Then the corresponding value of x was found from figure 3, y, from figure 2, and R_w, from

figure 5. The value of n is given by $n = y \sec \delta$. The value of M was obtained from the equation

$$M^2 = \csc^2(\epsilon - \delta) \frac{2 + (\gamma - 1) M_0^2 \sin^2\epsilon}{2\gamma M_0^2 \sin^2\epsilon - (\gamma - 1)}$$

and the value of δ, from the equation

$$\cot \delta = \tan \epsilon \left(\frac{\frac{\gamma + 1}{2} M_0^2}{M_0^2 \sin^2\epsilon - 1} - 1 \right) \tag{A17}$$

From the theory of oblique shock waves, furthermore,

$$\frac{p}{p_0} = \frac{2\gamma}{\gamma + 1} M_0^2 \sin^2\epsilon - \frac{\gamma - 1}{\gamma + 1} \tag{A18}$$

$$\Pi = \left(\frac{\gamma + 1}{2} \right)^{\frac{\gamma+1}{\gamma-1}} \left(\frac{M_0^2 \sin^2\epsilon}{1 + \frac{\gamma - 1}{2} M_0^2 \sin^2\epsilon} \right)^{\frac{\gamma}{\gamma-1}} \left(\frac{1}{\gamma M_0^2 \sin^2\epsilon - \frac{\gamma - 1}{2}} \right)^{\frac{\gamma}{\gamma-1}} \tag{A19}$$

The derivatives with respect to ϵ that appear in equations (A14) to (A16) were found by differentiating equations (A17) to (A19):

$$\frac{d\delta}{d\epsilon} = \sin^2\delta \left[\frac{(\gamma + 1) M_0^4 \sin^2\epsilon}{\left(M_0^2 \sin^2\epsilon - 1\right)^2} - \frac{\left(\frac{\gamma + 1}{2}\right) M_0^2 \sec^2\epsilon}{M_0^2 \sin^2\epsilon - 1} + \sec^2\epsilon \right]$$

$$\frac{d \log p}{d\epsilon} = \frac{2\gamma M_0^2 \sin \epsilon \cos \epsilon}{\gamma M_0^2 \sin^2\epsilon - \frac{\gamma - 1}{2}}$$

$$\frac{d \log \Pi}{d\epsilon} = \frac{2\gamma}{\gamma - 1} M_0^2 \sin \epsilon \cos \epsilon \left(\frac{1}{M_0^2 \sin^2\epsilon} - \frac{1}{\frac{2}{\gamma - 1} + M_0^2 \sin^2\epsilon} - \frac{1}{\gamma M_0^2 \sin^2\epsilon - \frac{\gamma - 1}{2}} \right)$$

APPENDIX B

DETERMINATION OF STREAMLINES AND FLOW VARIABLES FROM DENSITY

The flow field behind the curved shock wave (fig. 2) is rotational. The variation in the slope of the shock wave is known (fig. 3), however, as is the density in the flow field (fig. 6). The problem is to determine, from these known quantities, the streamlines and the values of flow variables other than density. The method that was used was to choose an element of arc on the shock wave, to calculate the average change in stagnation density across the element of arc, and then to construct the stream tube step by step in such a way that continuity was satisfied. The cross-sectional area of an annular stream tube is

$$A = 2\pi y\, \Delta n$$

Continuity requires that the equation

$$y\, \Delta n = \frac{\rho_0 V_0 y_0 (\Delta n)_0}{\rho V}$$

be satisfied. The velocity V can be expressed in terms of density and Mach number by means of the equation

$$V = Ma_s \frac{a}{a_s}$$

in which a_s/a is given by

$$\frac{a_s}{a} = \left(1 + \frac{\gamma - 1}{2} M^2\right)^{1/2}$$

in which a_s is a constant and in which M is given by

$$\frac{\rho_s}{\rho} = \left(1 + \frac{\gamma - 1}{2} M^2\right)^{\frac{1}{\gamma - 1}}$$

where ρ_s is a function of the shock-wave angle and free-stream conditions. The quantity $y\, \Delta n$ can consequently be expressed in terms of known quantities in the free stream, the shock-wave angle, and density behind the shock wave at Δn.

If one side of a stream tube is known, the other side can be located. First, the other side is drawn approximately. Then, the center line of the stream tube is drawn approximately. With the known

value of density and the measured value of y at the intersection of the center line and a known contour of constant ρ/ρ_0, the value of Δn is calculated. Then a line perpendicular to the center line is drawn through the point. Where this line intersects the known side of the stream tube, the value of y is measured. One half of the vertical projection of the calculated Δn is added to this value of y to give a closer approximation of y for recalculating Δn. The new Δn is used to obtain a better approximation for y and so on until the process converges.

The procedure was to obtain first the stream tube adjacent to the axis of symmetry and the surface of the sphere. The other stream tubes were than located by applying to each in turn the process described. A check which showed that any cumulative errors were negligibly small was the fact that the method gave deflection angles of the streamlines at the shock wave that agreed well with the theoretical values.

REFERENCES

1. Crocco, Luigi: Singolarità della corrente gassosa iperacustica nell'intorno di una prora a diedro. L'Aerotecnica, vol. XVII, fasc. 6, June 1937, pp. 519-534.

2. Maccoll, J. W.: Investigation of Compressible Flow at Sonic Speeds. Theoretical Res. Rep. No. 7/46, Armament Res. Dept., British Ministry of Supply, Sept. 1946.

3. Drougge, Georg: The Flow around Conical Tips in the Upper Transsonic Range. Rep. No. 25, Aero. Res. Inst. of Sweden (Stockholm), 1948.

4. Guderley, K. Gottfried: Considerations of the Structure of Mixed Subsonic-Supersonic Flow Patterns. Tech. Rep. No. F-TR-2168-ND, Air Materiel Command, U. S. Air Force, Oct. 1947.

5. Thomas, T. Y.: First Approximation of Pressure Distribution on Curved Profiles at Supersonic Speeds. Proc. Nat. Acad. Sci., vol. 35, no. 11, Nov. 1949, pp. 617-627.

6. Lin, C. C., and Rubinov, S. I.: On the Flow behind Curved Shocks. Jour. Math. and Phys., vol. XXVII, No. 2, July 1948, pp. 105-129.

7. Dugundji, John: An Investigation of the Detached Shock in Front of a Body of Revolution. Jour. Aero. Sci., vol. 15, no. 12, Dec. 1948, pp. 699-705.

8. Busemann, Adolf: A Review of Analytical Methods for the Treatment of Flows with Detached Shocks. NACA TN 1858, 1949.

9. Ferri, Antonio: Method for Evaluating from Shadow or Schlieren Photographs the Pressure Drag in Two-Dimensional or Axially Symmetrical Flow Phenomena with Detached Shock. NACA TN 1808, 1949.

10. Moeckel, W. E.: Approximate Method for Predicting Form and Location of Detached Shock Waves ahead of Plane or Axially Symmetric Bodies. NACA TN 1921, 1949.

11. Ladenburg, R., Van Voorhis, C. C., and Winckler, J.: Interferometric Study of Supersonic Phenomena. Part II: The Gas Flow around Various Objects in a Free Homogeneous Supersonic Air Stream. NAVORD Rep. 93-46, Sept. 2, 1946.

12. Heberle, Juergen W., Wood, George P., and Gooderum, Paul B.: Data on Shape and Location of Detached Shock Waves on Cones and Spheres. NACA TN 2000, 1950.

13. Gooderum, Paul B. and Wood, George P.: Density Fields around a Sphere at Mach Numbers 1.30 and 1.62. NACA TN 2173, 1950.

14. Ferri, Antonio: Application of the Method of Characteristics to Supersonic Rotational Flow. NACA Rep. 841, 1946. (Formerly NACA TN 1135.)

NACA

L-64902

Figure 1.- Interferogram of flow around sphere at Mach number 1.62.

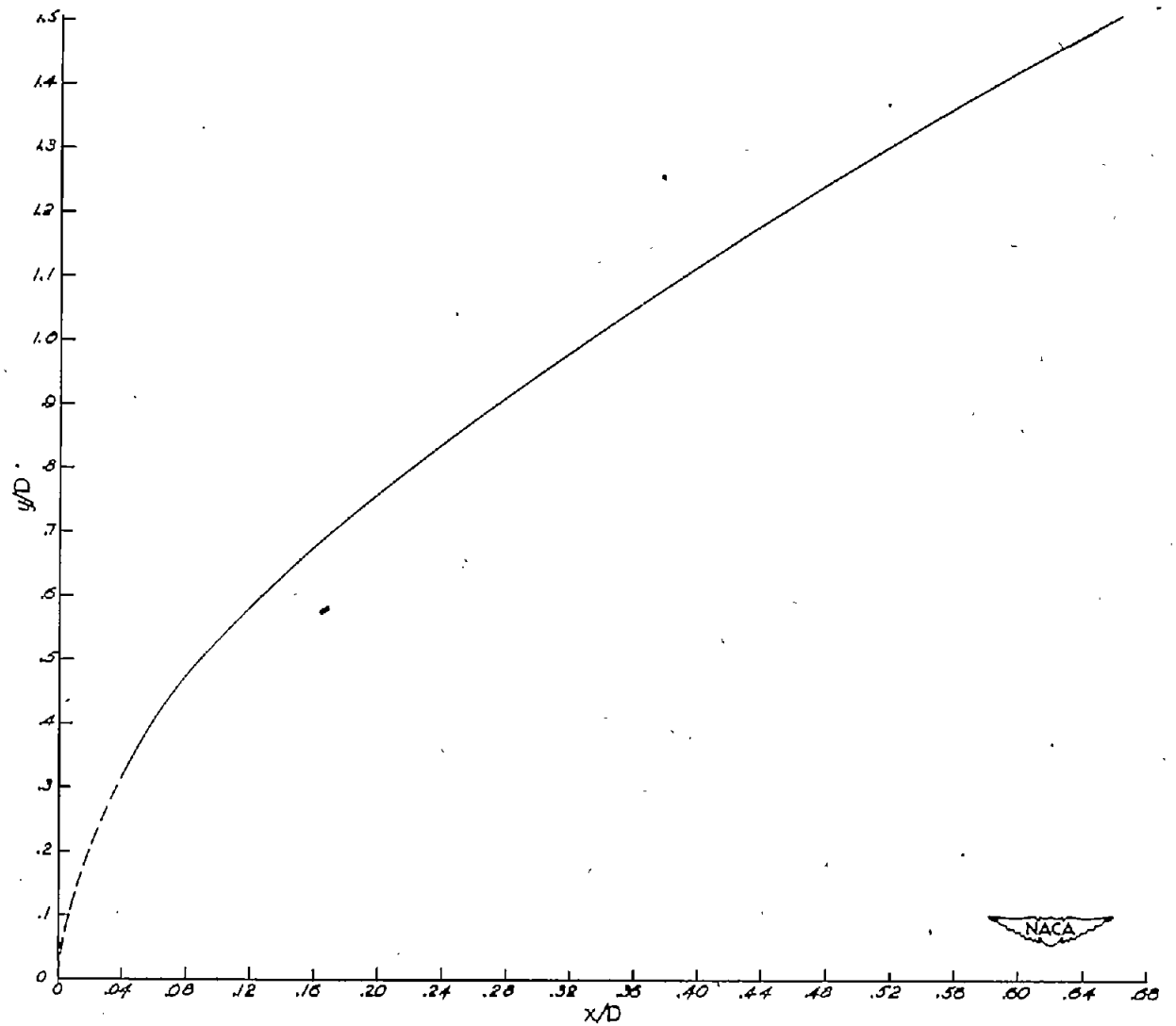

Figure 2.- Location of shock wave.

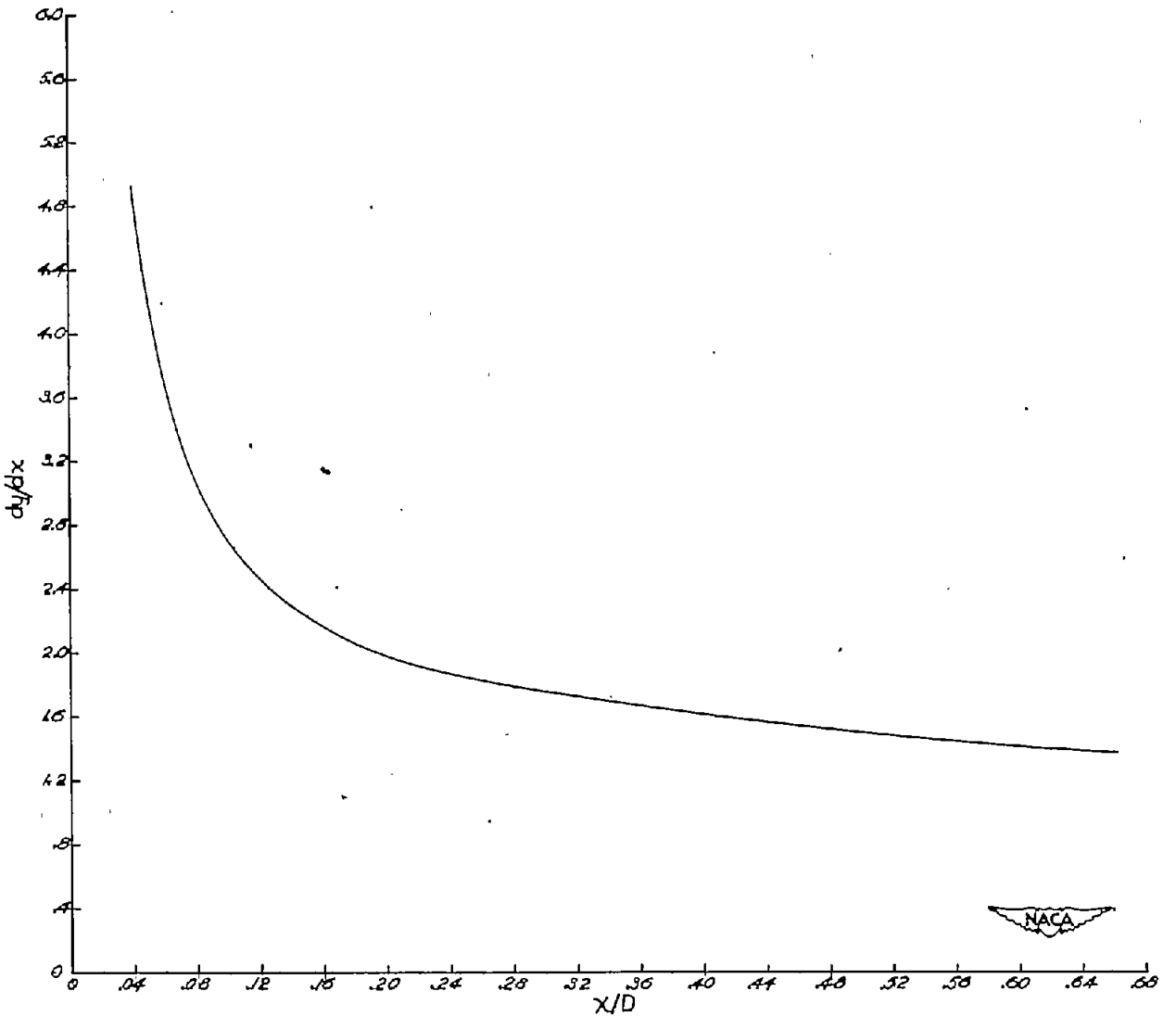

Figure 3.- Variation of slope of shock wave.

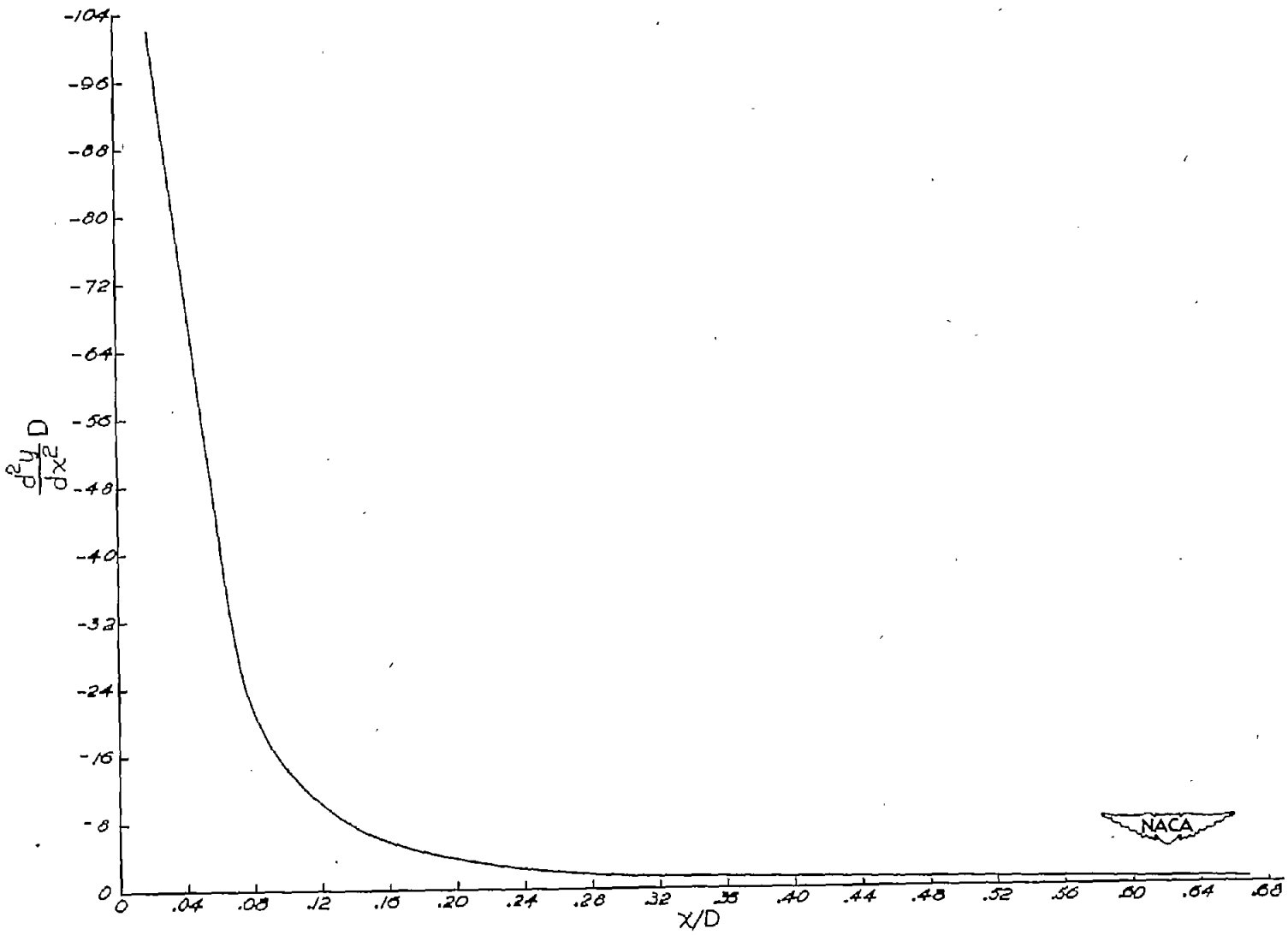

Figure 4.- Variation of second derivative of shock wave.

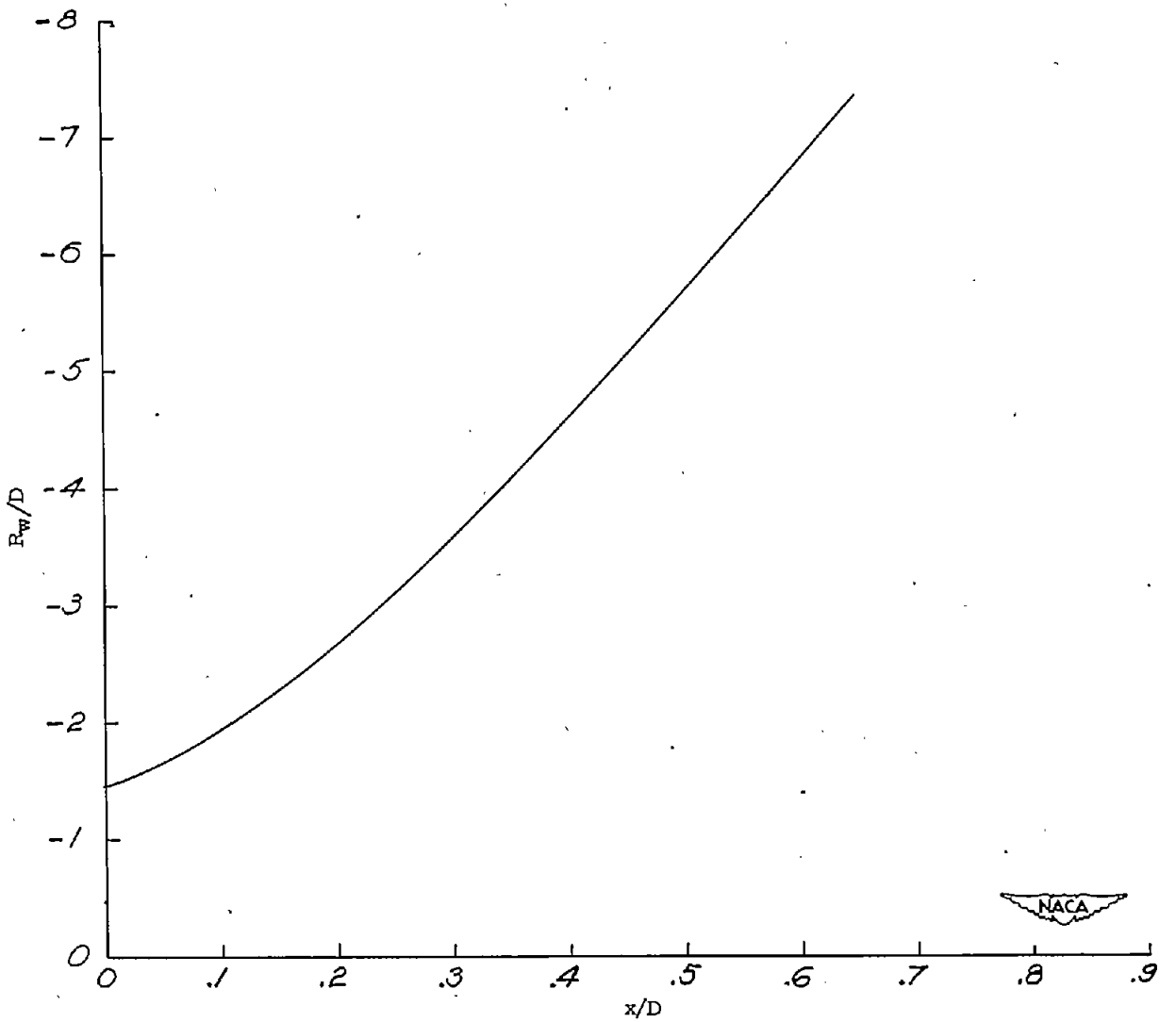

Figure 5.- Variation of radius of curvature along shock wave.

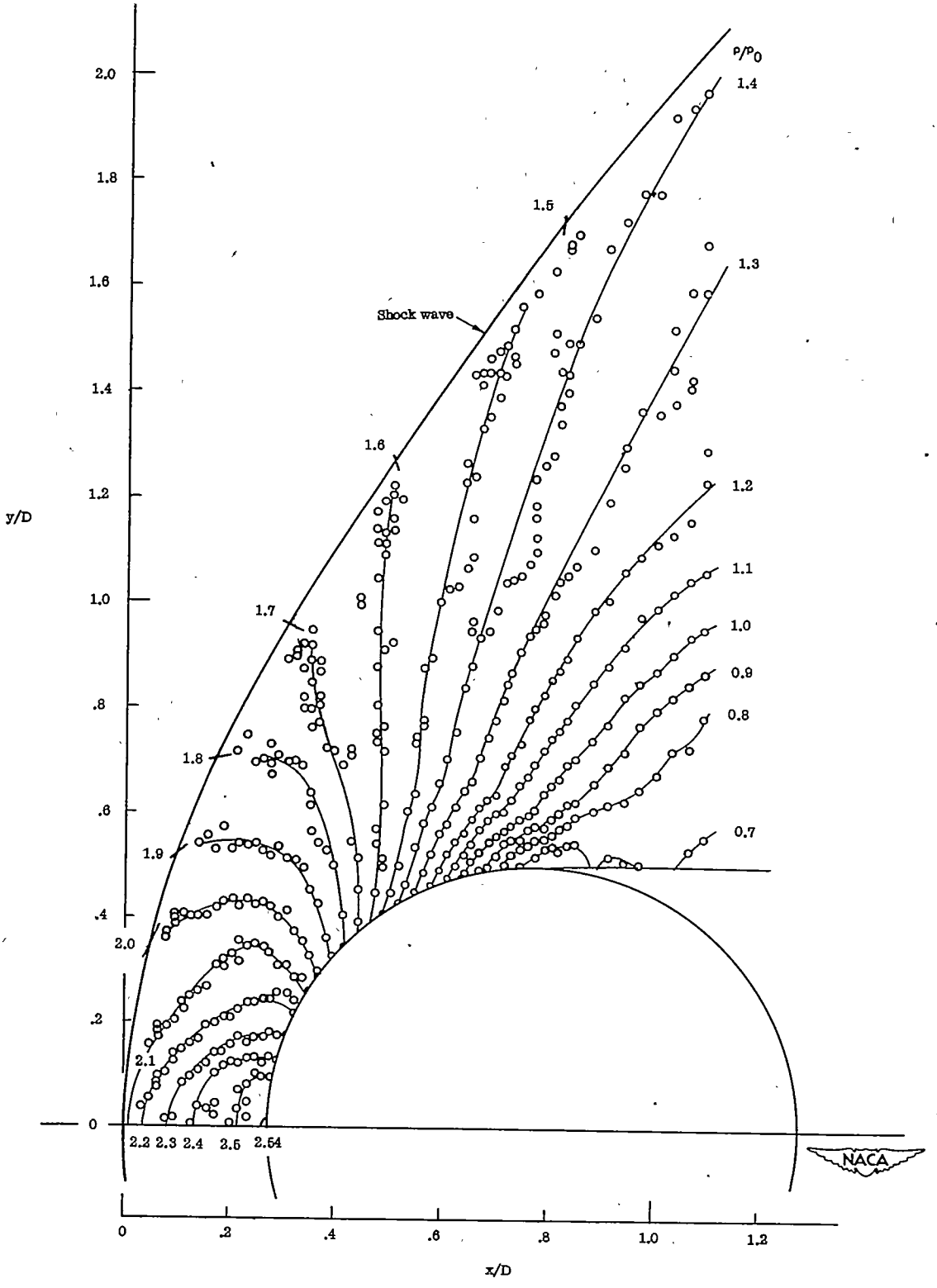

Figure 6.- Contours of constant ratio of density to free-stream density obtained from interferogram. (From fig. 5(b) of reference 13.)

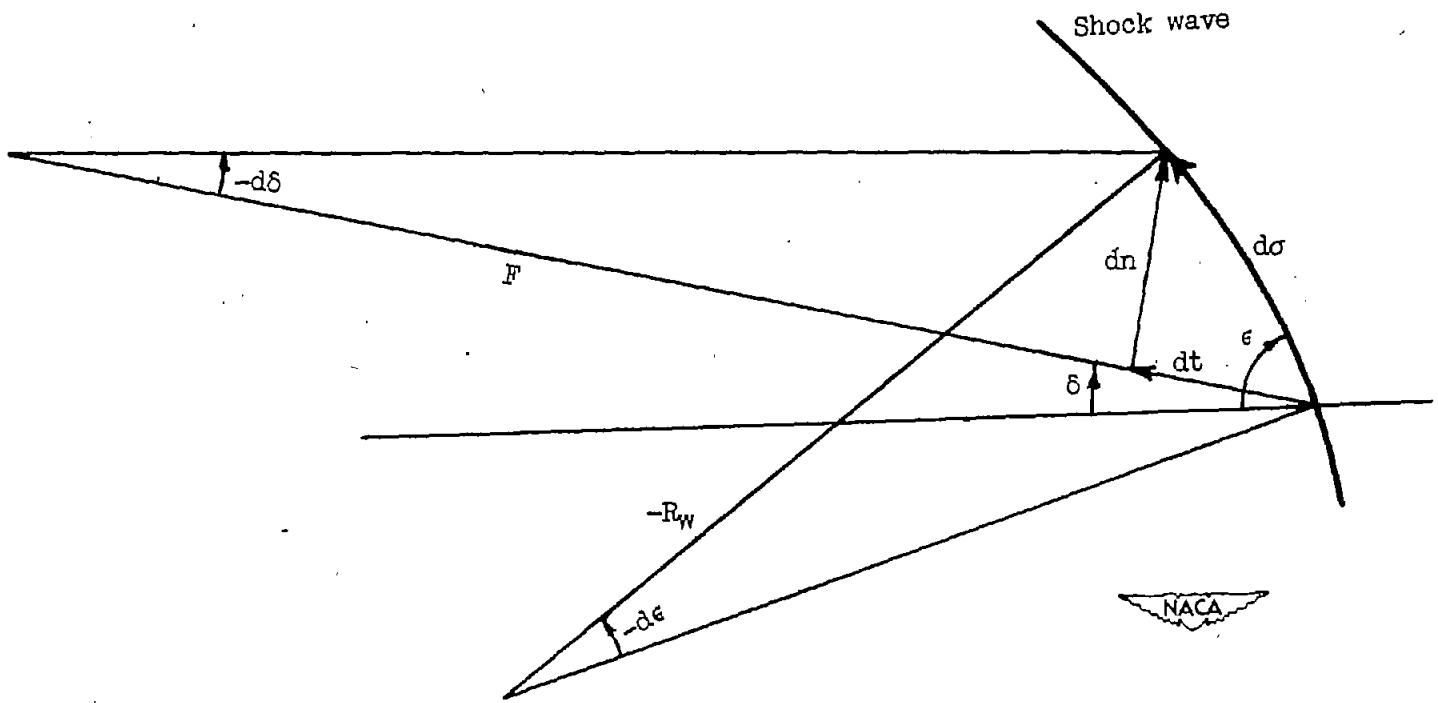

Figure 7.- Focus of initial tangents of streamlines.

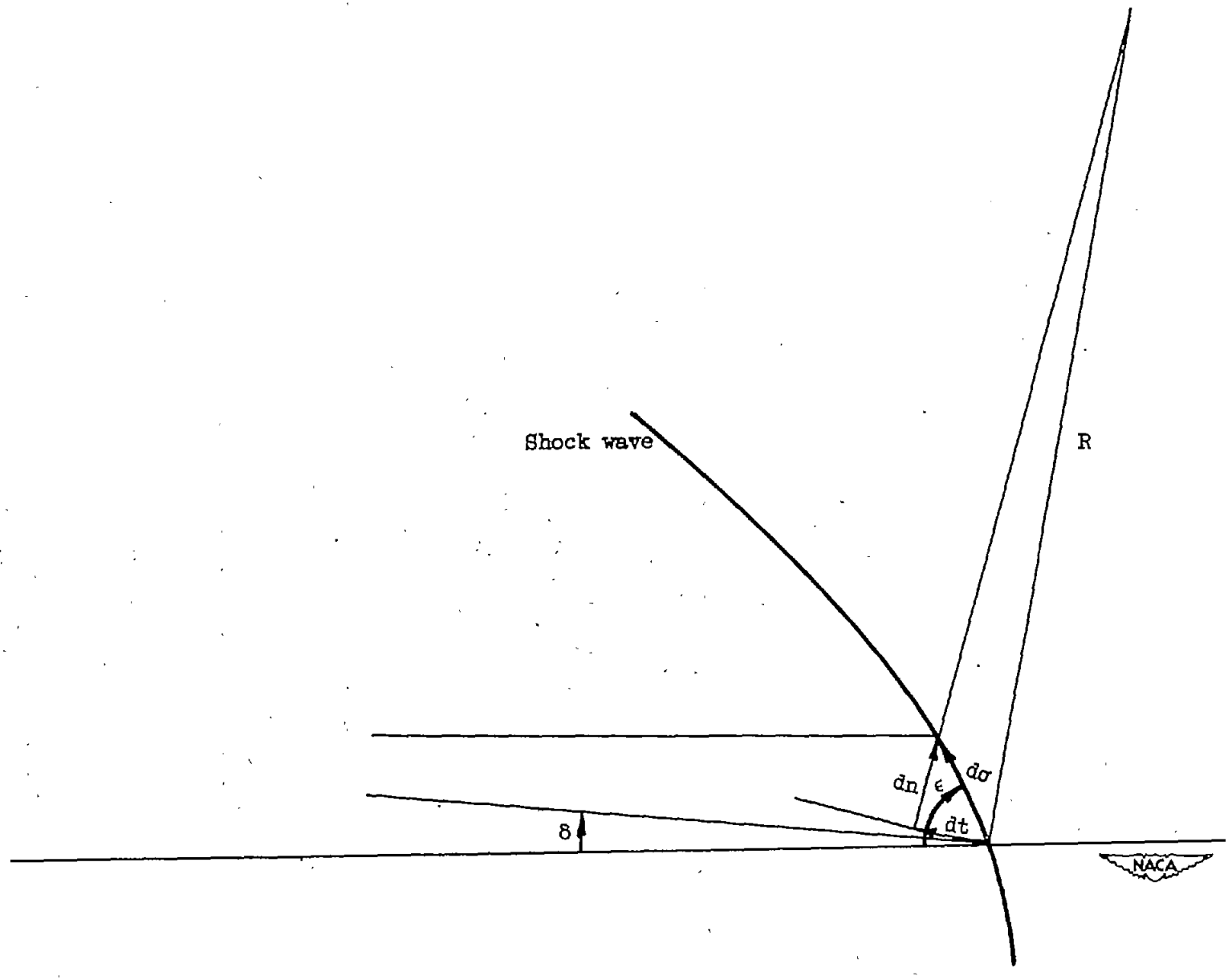

Figure 8.- Initial curvature of a streamline.

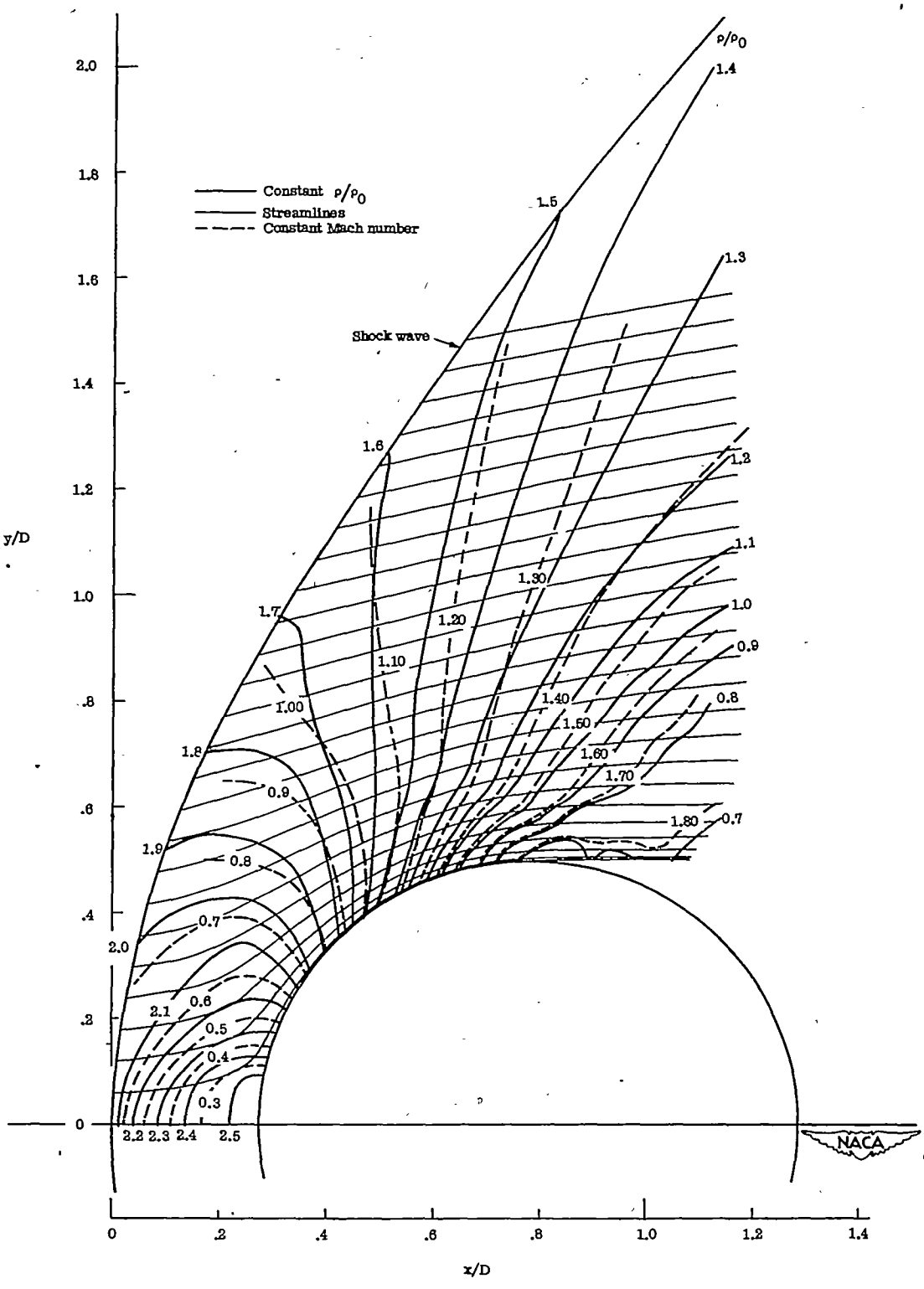

Figure 9.- Streamlines and contours of constant Mach number derived from continuity and contours of constant density.

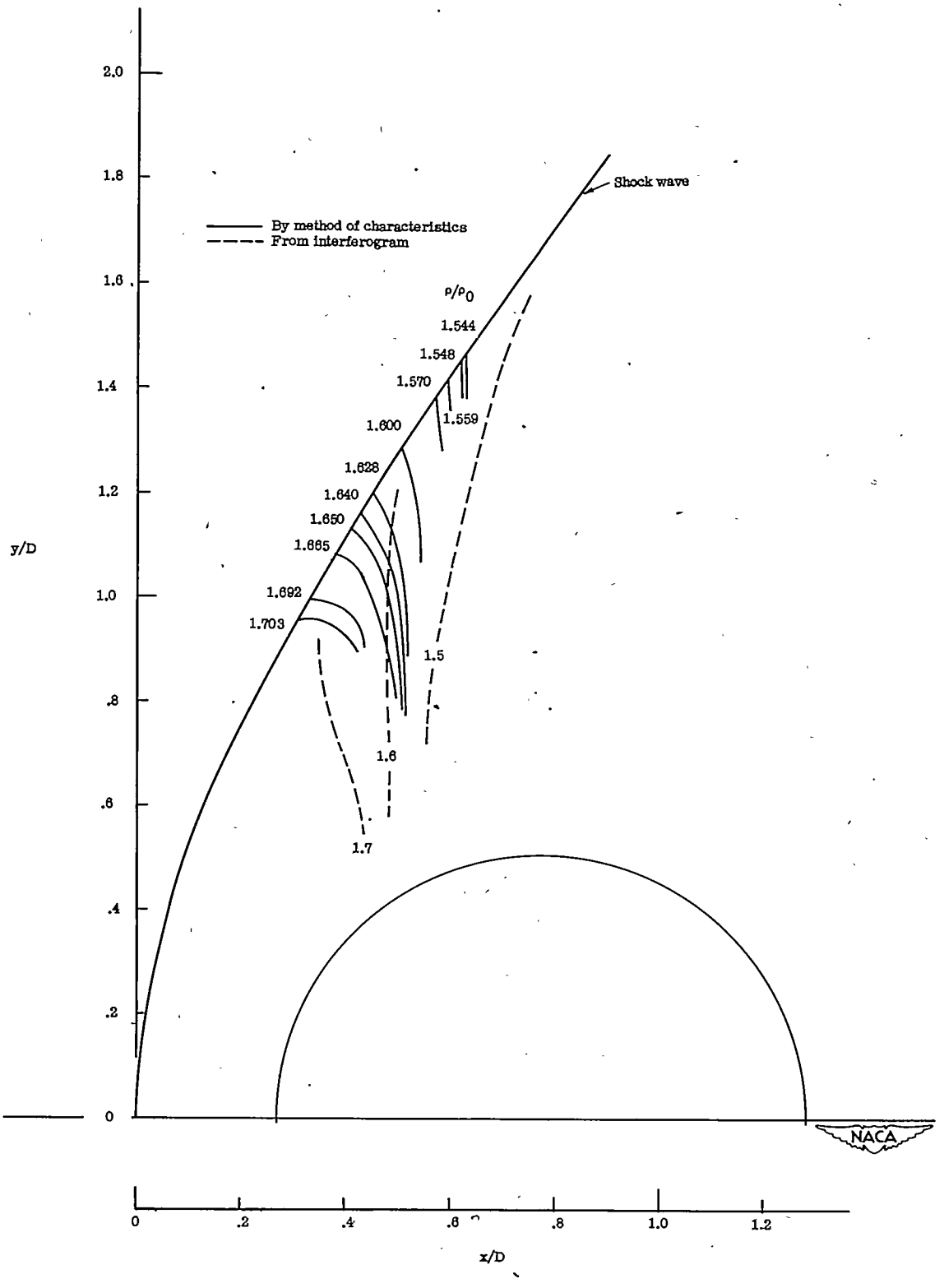

(a) Contours of constant ratio of density to free-stream density.

Figure 10.- Results obtained by method of characteristics and by interferometry.

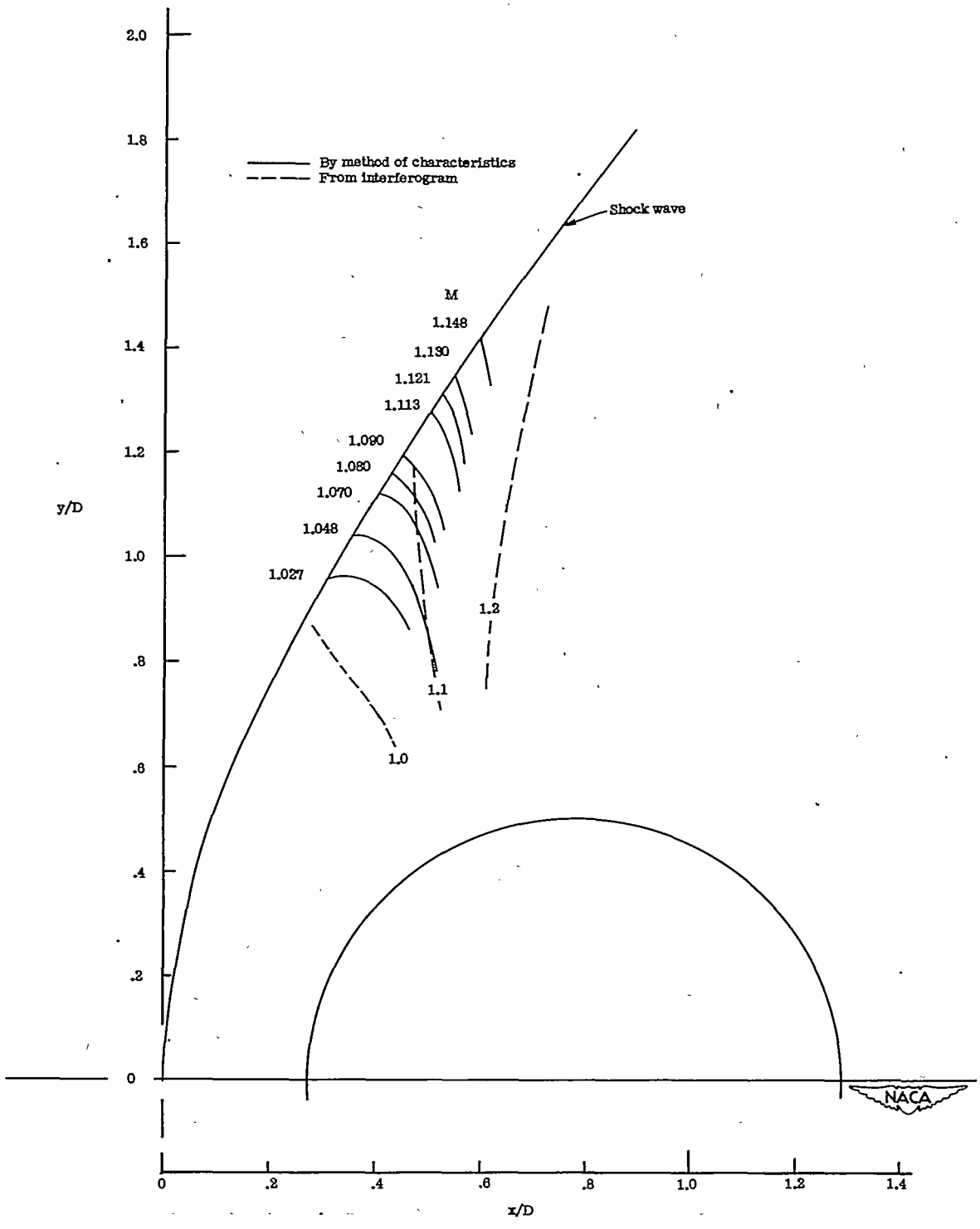

(b) Contours of constant Mach number.

Figure 10.- Continued.

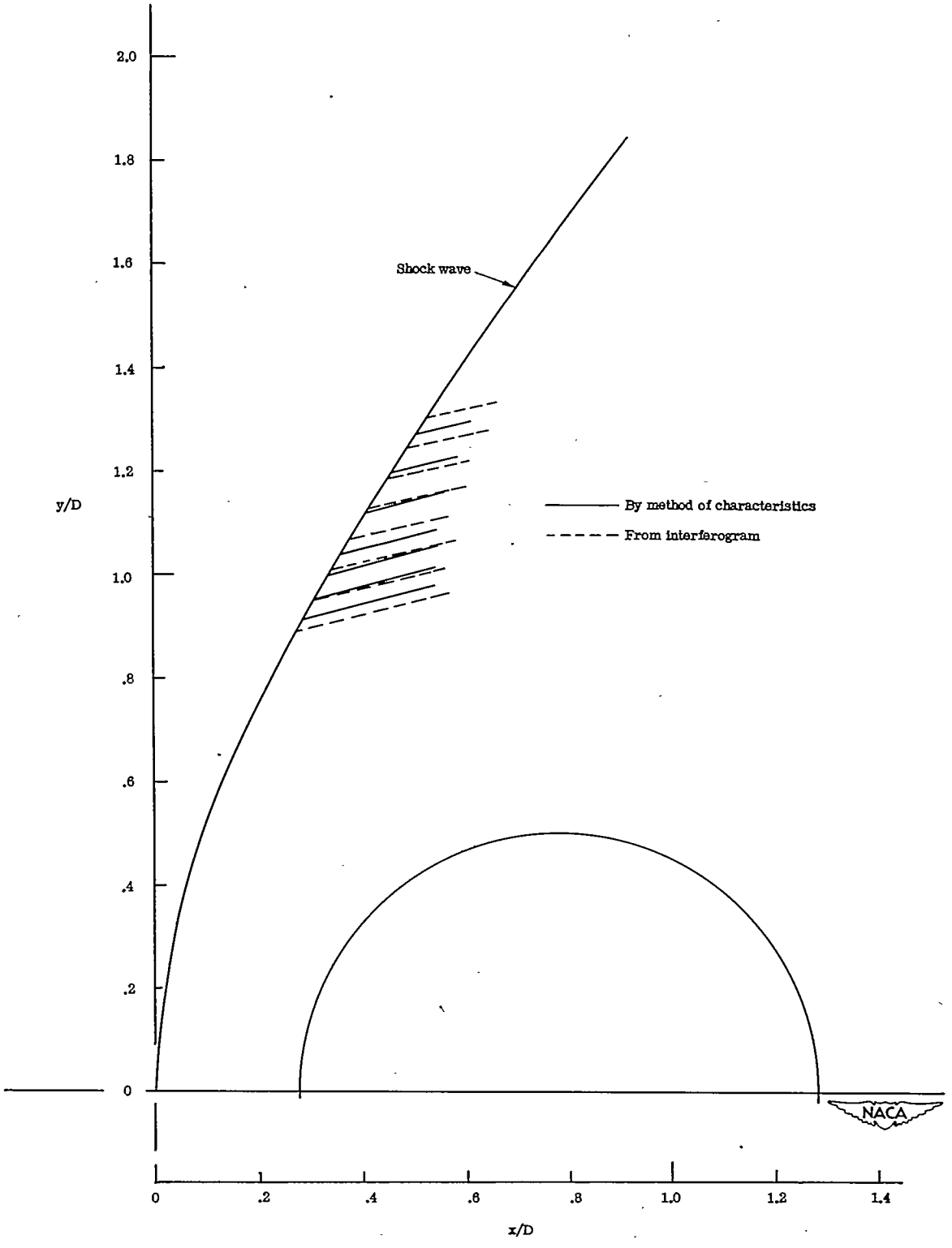

(c) Streamlines.

Figure 10.- Concluded.

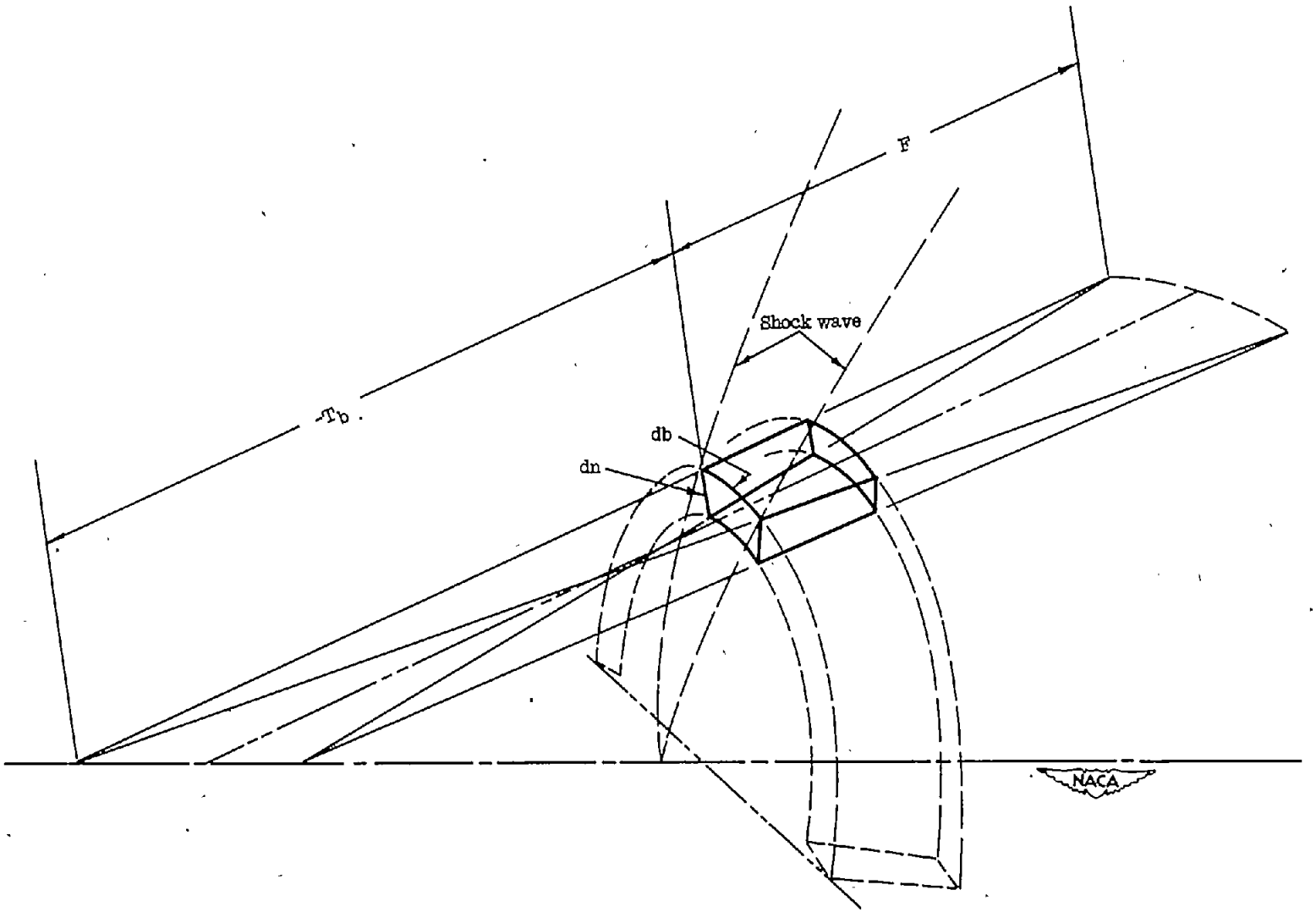

Figure 11.- Element of annular stream tube.

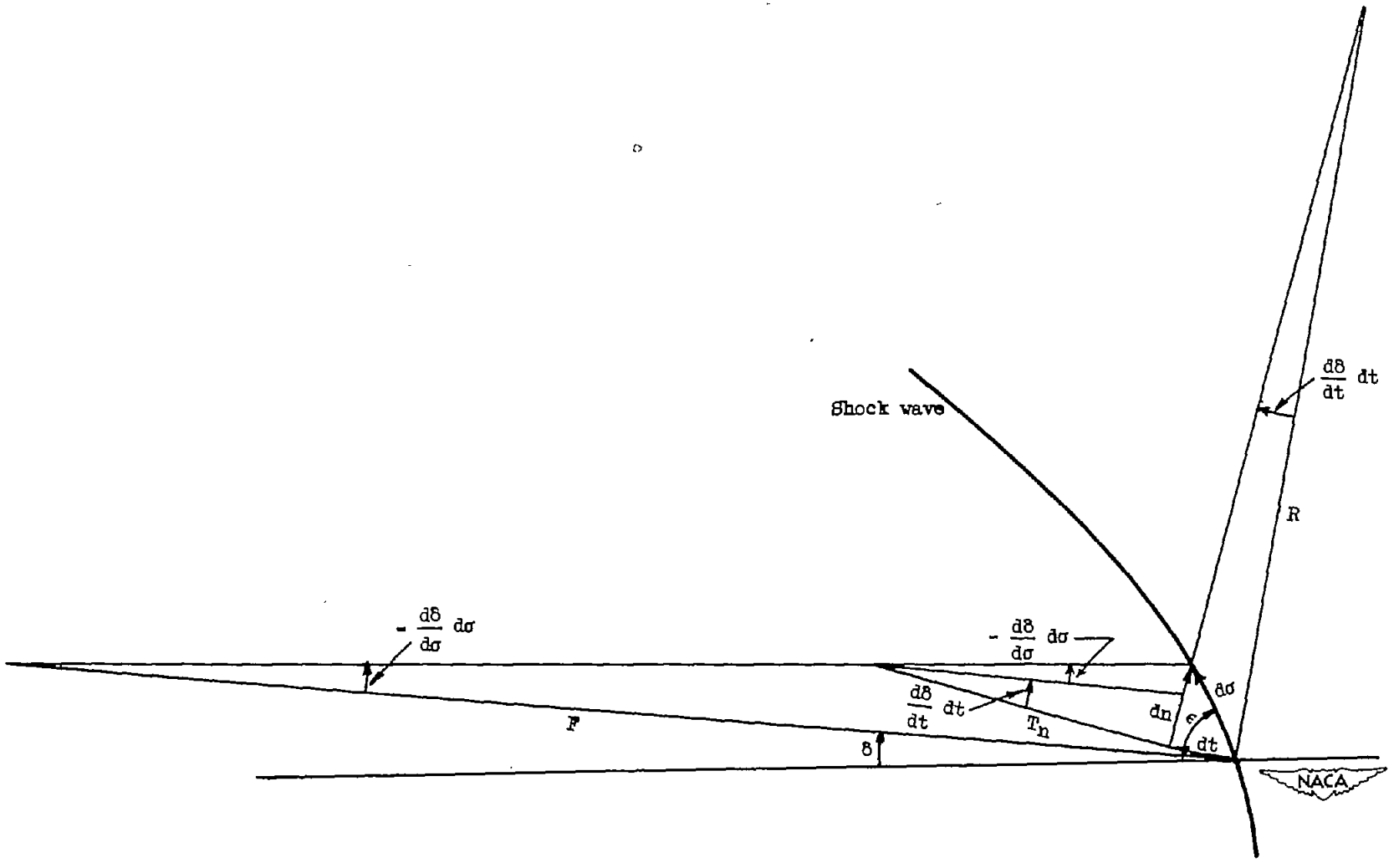

Figure 12.- Sketch showing taper of element of stream tube in plane of normal.

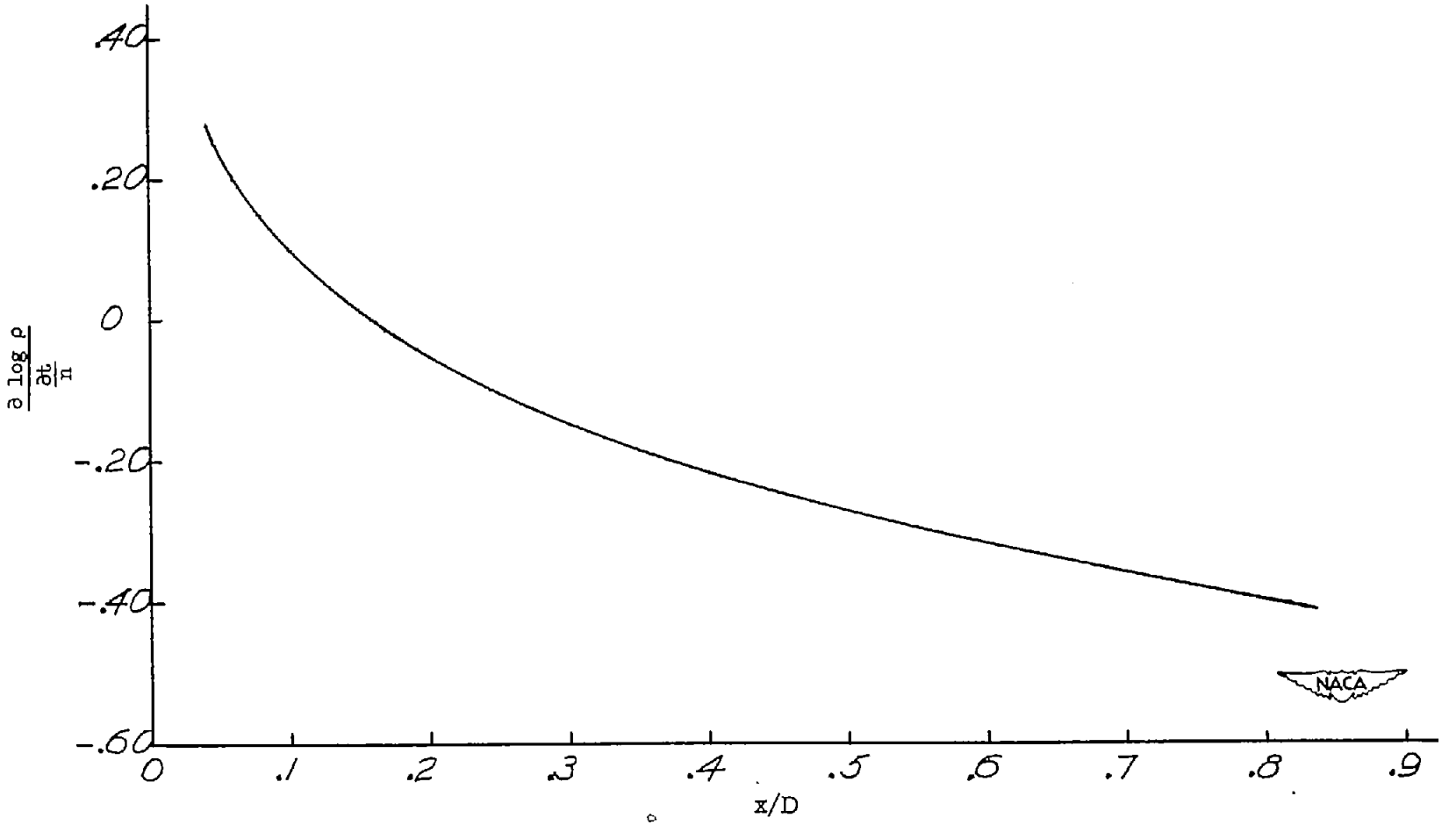

(a) Tangential derivative.

Figure 13.- Variation of density derivatives with x/D.

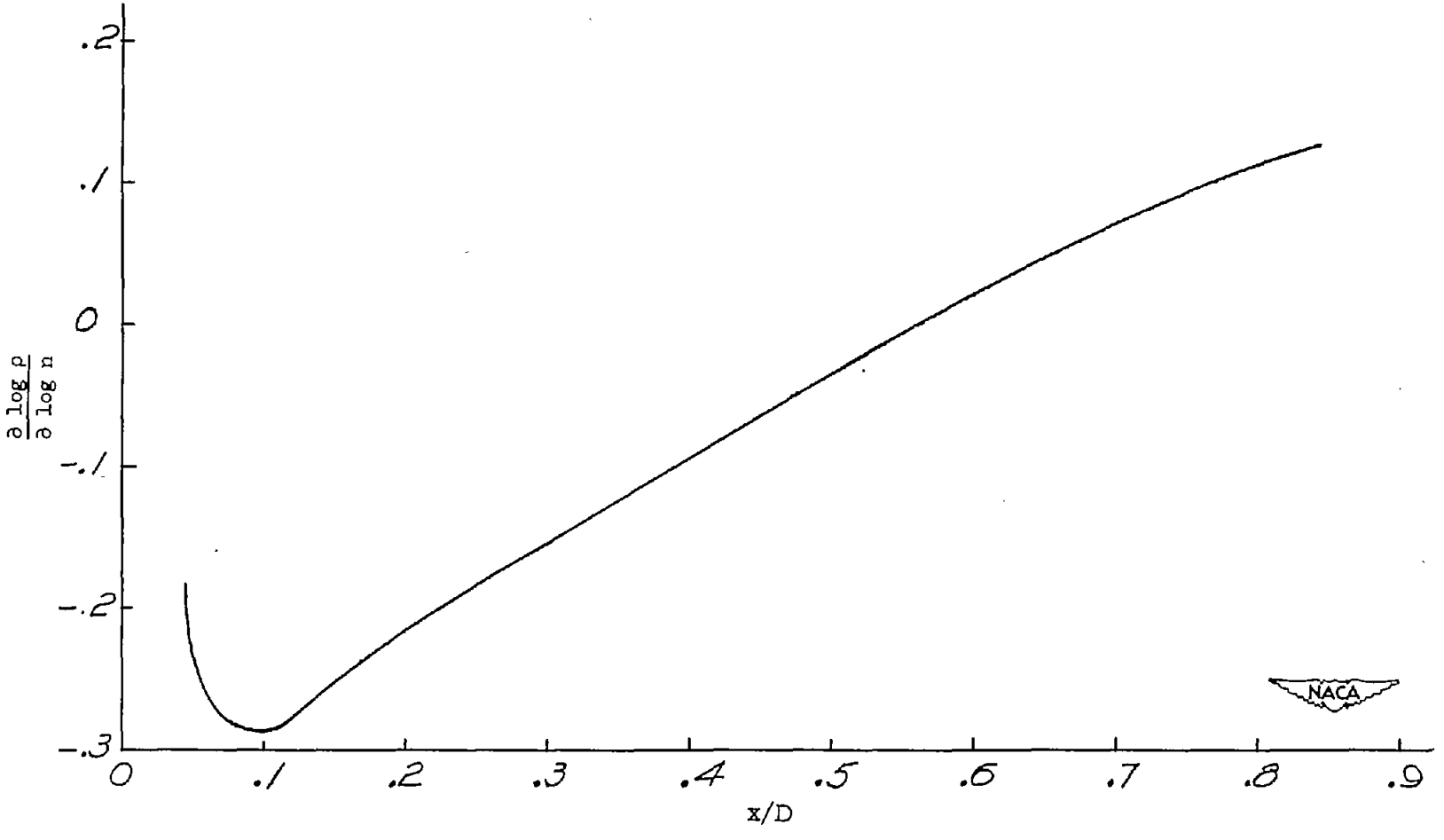

(b) Normal derivative.

Figure 13.- Concluded.

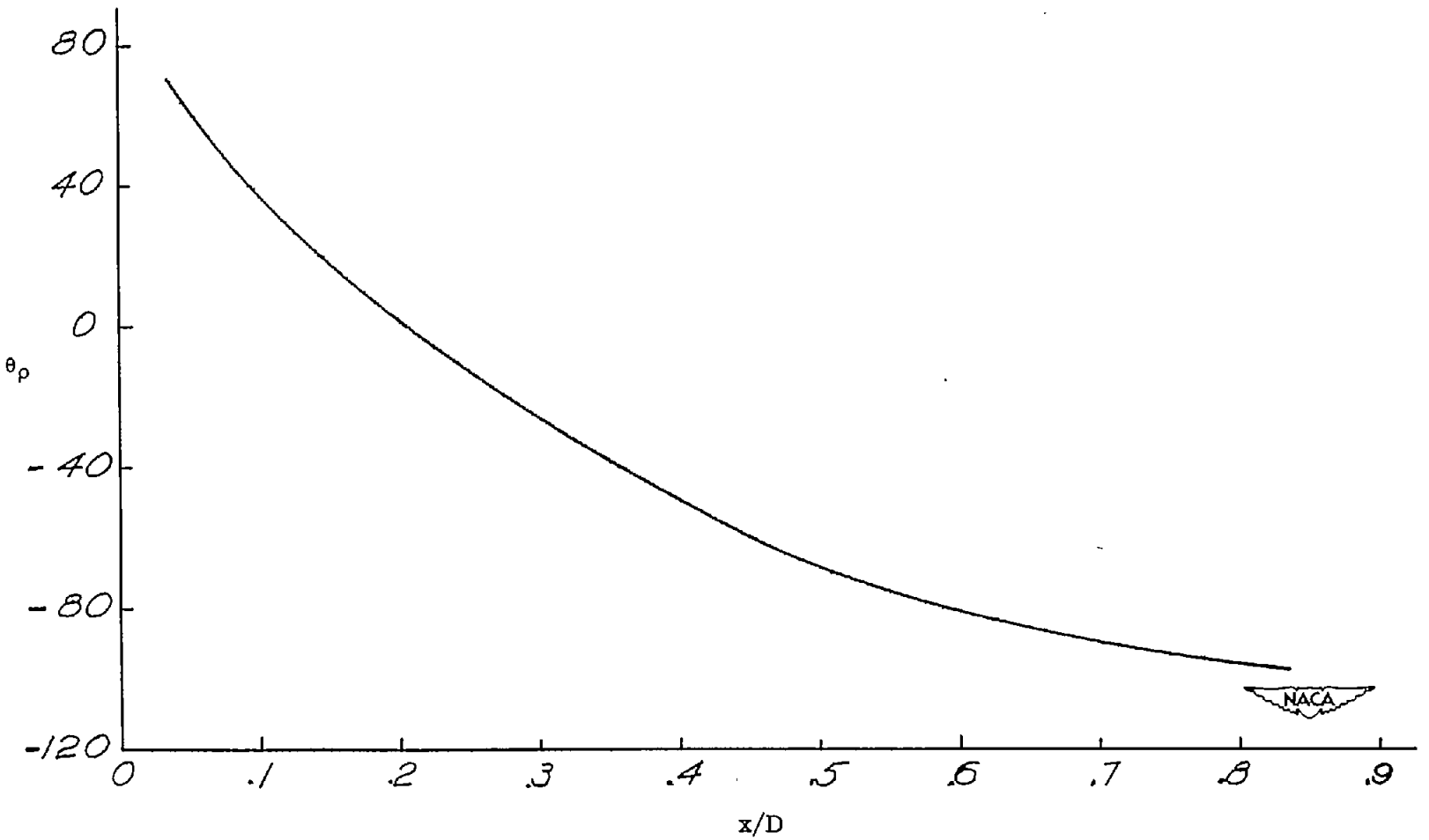

Figure 14.- Initial angle of density contour as a function of x/D.